

# High-Reynolds-number turbulence in a shear-free boundary layer: revisiting the Hunt–Graham theory

By JACQUES MAGNAUDET

Institut de Mécanique des Fluides de Toulouse, UMR 5502,  
2 avenue Camille Soula, 31400 Toulouse, France

(Received 11 July 2002 and in revised form 21 January 2003)

The capability of rapid distortion theory to predict the long-time evolution of shearless turbulence close to an impermeable surface has been seriously questioned in recent years. However, experiments and large-eddy simulations performed at high Reynolds number show that second-order turbulence statistics follow closely the predictions of the theory elaborated by Hunt & Graham (1978). To clarify this issue, a theoretical analysis is carried out in order to determine the relative magnitude of the vortical corrections which were not taken into account in the original theory. By evaluating the various terms of the enstrophy balance in the near-surface region, it is shown that this relative magnitude is a decreasing function of the turbulent Reynolds number, an argument reconciling most existing results. Hence the Hunt & Graham theory appears to be a leading-order approximation capable of describing short- and long-time evolutions of shear-free boundary layers in the limit of large Reynolds number. The expression for the pressure fluctuation corresponding to this approximation is then derived and approximate Reynolds stress budgets are obtained. These budgets are used to predict and discuss the characteristics of the intercomponent energy transfer near a flat surface in both time-decaying and spatially decaying turbulence. In agreement with available results, predictions reveal that tangential velocity components transfer energy towards the normal component in the former case, while they generally receive energy from this component in the latter case.

---

## 1. Introduction

Turbulence near impermeable surfaces is of central importance in both engineering and geophysical flows and has been a constant subject of investigation for almost a century. While turbulence dynamics in the near-surface region are often dominated by effects of shear, shear-free turbulent boundary layers are relevant to many physical situations. This is especially the case in gas–liquid flows when the liquid is driving the whole motion. In such situations, effects of surface boundary conditions are not obscured by those related to the existence of a mean shear and become much more prominent than in wall-bounded shear flows. In particular, provided the incoming turbulence is isotropic, the boundary conditions are entirely responsible for turbulence anisotropy in the boundary layer.

The canonical situation in which homogeneous isotropic turbulence evolves in the presence of a flat surface has been investigated theoretically, experimentally and numerically. However, despite significant effort, no general agreement on the basic concepts describing the effects of the surface has been reached so far. Most of the open

questions and controversies go back to the works of Hunt & Graham (1978) and Perot & Moin (1995a) (hereinafter referred to as HG and PM, respectively). Using the techniques of rapid distortion theory (RDT), HG derived a theoretical model describing the inviscid processes at work in a turbulent shear-free boundary layer. Basically this model describes how an isotropic turbulent flow responds instantaneously to the insertion of an impermeable surface. Owing to incompressibility, this instantaneous response is obtained by adding an irrotational component to the initial turbulent velocity field, so as to satisfy the kinematic boundary condition at the surface. This irrotational contribution represents the image of eddies with respect to the surface; its evaluation in spectral space allows various statistics characterizing the short-time response of the turbulent flow to be evaluated. One of the main predictions of the HG theory is that the tangential turbulent intensities increase at the expense of the normal ones near the surface, a feature frequently interpreted as a traceless energy transfer between the three velocity components.

The HG model was initially derived to explain the experimental results obtained by Uzkan & Reynolds (1967) and Thomas & Hancock (1977) who studied grid turbulence convected by a uniform stream past a rigid wall moving with the free-stream speed. Their measurements showed that, within a surface layer whose thickness is about one integral length scale, velocity fluctuations normal to the wall are progressively damped as the distance to the wall decreases. The evolution of the tangential components was found to be more complex. In the low-Reynolds-number experiments of Uzkan & Reynolds (1967) (corresponding to a Reynolds number  $Re_T \approx 90$ , where  $Re_T$  is based on the turbulent kinetic energy per unit mass and dissipation rate of the free-stream turbulence), the tangential fluctuations decreased monotonically as the wall was approached, and HG attributed this behaviour to the fact that the thickness  $\delta_V$  of the viscous sublayer attached to the moving wall was a large fraction of the integral scale  $L_\infty$ . In contrast, in the high-Reynolds-number experiment of Thomas & Hancock (1977) ( $Re_T \approx 2000$ ),  $\delta_V$  was much smaller than  $L_\infty$  and the tangential fluctuations increased as the wall was approached, prior to decreasing to zero in the viscous sublayer; in particular, the streamwise r.m.s. velocity exhibited a marked peak in the wall-influenced region far downstream from the leading edge of the moving wall. Most experimental findings of Thomas & Hancock (1977) are predicted well by the HG theory and the low- and high-Reynolds-number evolutions were qualitatively recovered in a coarse large-eddy simulation (LES) performed by Biringen & Reynolds (1981).

More recently, Aronson, Johansson & Löfdahl (1997) performed an experiment similar to that of Thomas & Hancock at a moderate Reynolds number ( $Re_T \approx 380$ ). They observed a peak in the tangential fluctuations solely near the leading edge of the wall, whereas further downstream this peak disappeared almost completely. This evolution, which is not predicted by the HG theory, agrees with the results of direct numerical simulations (DNS) performed by PM in the case of freely evolving turbulence subjected to the sudden insertion of a solid wall, a situation which, by virtue of Taylor's hypothesis, is equivalent to that of grid turbulence convected past a moving wall. PM argued that the peak reported by Thomas & Hancock could be due to turbulence production by a residual mean shear, whereas Aronson *et al.* (1997) suggested that the frictional heating due to the moving belt could have contaminated the hot wire determinations of the streamwise velocity. The crucial point is that both investigations conclude that no maximum exists in the tangential r.m.s. velocities at large time, i.e.  $t/T \gg 1$  ( $t=0$  corresponds to the time at which the wall is inserted and  $T$  is the large-eddy turnover time), whereas the existence of

this maximum is one of the central predictions of the HG theory. Consequently these two recent investigations seriously question the validity of the HG theory at large time.

The mathematical assumptions used in the derivation of the original HG theory (see also Hunt 1984) suggest that its results apply only during the early stages of the flow, i.e.  $t/T \ll 1$ . Nevertheless, Hunt (1984) conjectured that the theory remains valid for larger time in steady shearless flows, provided dissipation is almost constant in the surface-influenced layer. He also suggested that for  $t/T > 1$ , the vorticity of small eddies changes owing to the stretching and compression produced by the impingement of large-scale motions on the surface, a nonlinear effect whose major consequence is to generate an additional increase of the tangential velocities as the surface is approached. The predictions of HG and Hunt (1984) have been compared with measurements performed in statistically steady flows produced in stirred-grid water tanks, either in the presence of a free surface (McDougall 1979; Brumley & Jirka 1987) or near a sharp density interface (Hannoun, Fernando & List 1988; Kit, Strang & Fernando 1997). Overall, the trends revealed by these experiments are consistent with the predictions of the HG theory. In particular Brumley & Jirka (1987) compared the vertical evolution of turbulent intensities, integral length scales and energy spectra with theoretical predictions and found a convincing agreement, except in the thin surface viscous sublayer where a strong reduction of the tangential fluctuations was observed, probably because of the contamination of the free surface by impurities. Hannoun *et al.* (1988) and Kit *et al.* (1997) also reported a general agreement with the HG predictions; however they observed that in the top part of the surface-influenced layer, the tangential intensities increased significantly more than predicted by the original theory, especially in the low-wavenumber range. This sharp increase was found to follow fairly well the predictions corresponding to Hunt's (1984) nonlinear correction.

A conceptually different explanation of the interactions between a freely evolving, initially homogeneous, isotropic turbulence and a non-deformable surface suddenly inserted in the flow was proposed by PM who put emphasis on the energy transfer between the three r.m.s. velocity components. They performed DNS at different Reynolds numbers ( $54 \leq Re_T \leq 134$  in most cases) with three different types of boundary. The first was a permeable membrane (i.e. only the tangential velocities were forced to vanish), while the other two were a shear-free surface (also studied numerically in great detail by Walker, Leighton & Garza-Rios 1996, hereinafter referred to as WLGR), and a solid wall. To analyse near-surface interactions, PM defined two types of turbulent structures, 'splats' and 'anti-splats', which are easily detected in computations as well as in recent experiments performed in open-channel flows (e.g. Rashidi 1997 and Nagaosa 1999). The splats, also referred to as upwellings, patches or updraughts in other studies (Pan & Banerjee 1995; Rashidi 1997; Kumar, Gupta & Banerjee 1998), are blobs of fluid impinging on the surface. Such impingements produce stagnation points characterized by a negative gradient of the normal velocity. Since stagnation points are associated with high pressure levels, such events provide a negative contribution to the normal component of the pressure-strain correlation and they transfer momentum to the motion parallel to the surface. Then, when the tangential motions resulting from the impingement of two neighbouring updraughts meet, another stagnation point where the normal velocity experiences a positive gradient is produced. This results in fluid motion away from the surface, an event called an anti-splat by PM (also referred to as downdraught by other authors). As pointed out by PM, since downdraughts contribute positively

to the normal component of the pressure–strain correlation, the coexistence of both types of structures implies that the net (averaged) intercomponent energy transfer is determined by the imbalance between updraughts and downdraughts, rather than by the updraughts themselves as previously believed.

In their computations, PM observed that the intercomponent energy transfer was significantly weaker close to a shear-free surface than close to a solid wall or a permeable membrane. Since viscous effects are much stronger in the latter two configurations than in the former one (for a given Reynolds number), this led them to the conclusion that the strength of near-surface viscous effects determines the rate of imbalance between splats and anti-splats. This view is completely different from that provided by the HG theory where the increase of the tangential turbulent intensities at the expense of the normal ones is due to a purely kinematic process. That the imbalance between updraughts and downdraughts governs intercomponent energy transfer was subsequently confirmed by WLGR and Nagaosa (1999). However, both groups disagree with PM about the cause of this imbalance, which WLGR attribute to the anisotropy induced by the vanishing of the normal r.m.s. velocity on the surface (a kinematic process), whereas the explanation of Nagaosa, more specific to open-channel flow, is based on the interaction of quasi-streamwise vortices with the surface. Further, PM noticed two important features in the particular case of a shear-free surface. First, they showed that the tangential turbulent intensities exhibit a peak at the surface (also observed by WLGR), the relative intensity of which (normalized by the free-stream intensity) increases with time. They suggested that this peak is not related to that predicted by the HG theory, being due rather to the fact that turbulence decays faster far from the surface than close to it because dissipation is strongly reduced in the viscous sublayer. Second, they noticed that owing to the smallness of pressure–strain correlations close to the surface, the evolution of the turbulent intensities is essentially governed by a balance between dissipation, viscous diffusion and turbulent transport. Since none of these terms appears in the HG analysis, they concluded that this theory essentially provides the initial condition for the velocity field, but that the subsequent evolution has little to do with RDT predictions.

This overview shows that the present state of the art concerning the physics of shear-free turbulent boundary layers is quite controversial. Recently, Calmet & Magnaudet (2003) (hereinafter referred to as CM) reported results of a high-Reynolds-number LES in a statistically steady open-channel flow ( $Re_T \approx 800$ ). Since the anisotropy of the turbulence entering the surface-influenced region was moderate, detailed comparison of various second-order statistics with HG predictions was possible. Despite the residual anisotropy and the inhomogeneity of the underlying turbulence, this comparison revealed a close quantitative agreement on all second-order statistical quantities outside the viscous sublayer. This agreement gave us a strong motivation to revisit several aspects of the HG theory in order to clarify some of the controversies summarized above. This new look at the conditions of validity and implications of the existing theory is the essential goal of the present contribution. Our aim in this paper is to understand with the aid of approximate enstrophy and energy budgets what the main statistical effects of a flat surface on the underlying turbulence are, especially after many turnover times. Clarifying these effects and elucidating the controversy described above may have some bearing on turbulence modelling, since any model aimed at predicting second-order turbulence statistics near impermeable surfaces should reproduce the essential features of the fundamental situation considered here.

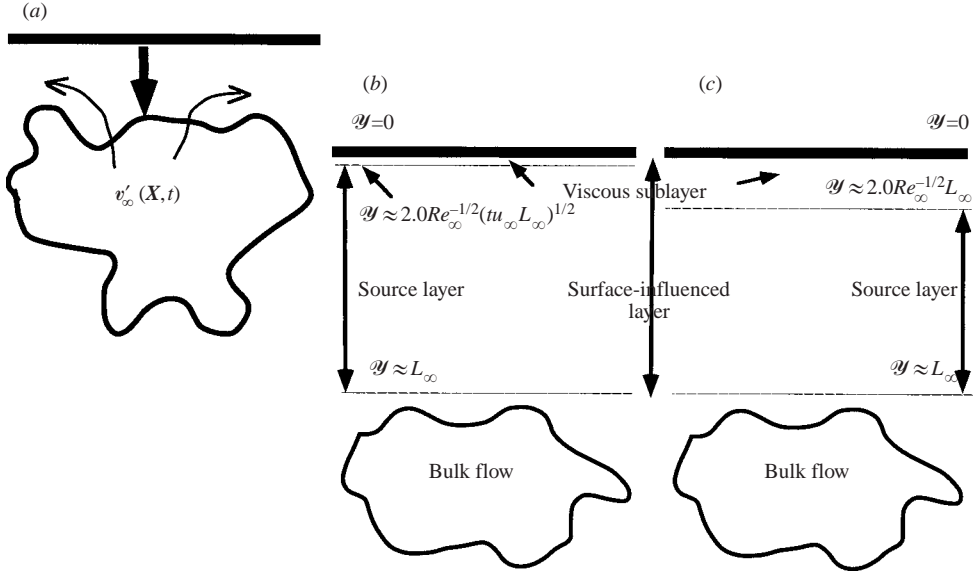


FIGURE 1. Sketch of the development of a turbulent shear-free boundary layer: (a) insertion of a flat surface at  $t = 0$ ; (b) two-layer structure at short time ( $t \ll L_\infty/u_\infty$ ); (c) two-layer structure at long time ( $t \gg L_\infty/u_\infty$ ).

The governing equations of the problem are derived and commented on in §2. In §3 we determine the magnitude of long-term corrections to the HG theory. We also derive the expression for the pressure fluctuation corresponding to the HG solution and the associated Reynolds stress budget. In §4 we examine the implications of the theory with respect to intercomponent energy transfer mechanisms in two reference situations, namely time-decaying (or freely evolving) turbulence, and spatially decaying turbulence. A summary and final remarks are given in §5. Some analytical extensions of the HG theory are also reported in Appendices A and B, whereas Appendix C re-examines the conditions of validity of Hunt's (1984) nonlinear correction.

## 2. Statement of the problem

### 2.1. Governing equations

Let us consider an incompressible turbulent flow in which a flat impermeable surface is suddenly inserted in the plane  $\mathcal{Y} = 0$  at time  $t = 0$  (figure 1a). The flow is assumed to satisfy conditions of statistical homogeneity along the tangential directions  $x$  and  $z$ . For simplicity we also assume that there is no mean flow or that the mean flow is independent of  $\mathcal{Y}$ , so that it can be accounted for by a suitable Galilean transformation. We denote by  $\mathbf{v}'(\mathbf{X}, t)$  and  $p'(\mathbf{X}, t)$  the velocity and pressure fluctuations at time  $t$  and position  $\mathbf{X} = (x, \mathcal{Y}, z)$ , and by  $\mathbf{v}_\infty(\mathbf{X}, t)$  and  $p_\infty(\mathbf{X}, t)$  the corresponding fields that would exist at time  $t$  if the surface were absent. The impermeable surface forces the normal velocity to satisfy the kinematic condition

$$\mathbf{v}' \cdot \mathbf{n} = 0 \quad \text{for } \mathcal{Y} = 0 \quad \text{and } t > 0, \quad (1)$$

where  $\mathbf{n}$  denotes the unit normal to the surface directed into the fluid. As is well known, the velocity field  $\mathbf{v}'(\mathbf{X}, t)$  may be written at any time  $t \geq 0$  in the form

(Batchelor 1967, p. 87)

$$\mathbf{v}'(\mathbf{X}, t) = \mathbf{v}_\infty(\mathbf{X}, t) + \nabla\Phi(\mathbf{X}, t) + \nabla \times \mathbf{A}(\mathbf{X}, t), \quad (2)$$

where  $\Phi$  is a scalar potential and  $\mathbf{A}$  is a vector potential subject to the solenoidality condition

$$\nabla \cdot \mathbf{A} = 0. \quad (3)$$

Decomposition (2) and condition (3) imply that the vorticity  $\boldsymbol{\omega}'(\mathbf{X}, t) = \nabla \times \mathbf{v}'(\mathbf{X}, t)$  is related to  $\boldsymbol{\omega}_\infty(\mathbf{X}, t) = \nabla \times \mathbf{v}_\infty(\mathbf{X}, t)$  through

$$\boldsymbol{\omega}' = \boldsymbol{\omega}_\infty - \nabla^2 \mathbf{A}. \quad (4)$$

Since  $\mathbf{v}'$  is divergence-free, the scalar potential satisfies the Laplace equation

$$\nabla^2 \Phi = 0. \quad (5)$$

From the transport equation of  $\boldsymbol{\omega}'$ , the governing equation of the vorticity disturbance  $\boldsymbol{\omega}_A = -\nabla^2 \mathbf{A}$  is found to be

$$\begin{aligned} \left( \frac{\partial}{\partial t} - \nu \nabla^2 \right) \boldsymbol{\omega}_A + (\mathbf{v}_\infty + \nabla\Phi + \mathbf{v}_A) \cdot \nabla \boldsymbol{\omega}_A - \boldsymbol{\omega}_A \cdot \nabla (\mathbf{v}_\infty + \nabla\Phi + \mathbf{v}_A) \\ + \mathbf{v}_A \cdot \nabla \boldsymbol{\omega}_\infty - \boldsymbol{\omega}_\infty \cdot \nabla \mathbf{v}_A = \boldsymbol{\omega}_\infty \cdot \nabla (\nabla\Phi) - \nabla\Phi \cdot \nabla \boldsymbol{\omega}_\infty, \end{aligned} \quad (6)$$

where  $\nu$  is the kinematic viscosity and  $\mathbf{v}_A = \nabla \times \mathbf{A}$  is the vortical velocity disturbance. At large  $\mathscr{Y}$ , the surface-induced disturbance vanishes, so that

$$\boldsymbol{\omega}_A \rightarrow \mathbf{0}, \quad (7a)$$

$$\|\nabla\Phi\| \rightarrow 0. \quad (7b)$$

The remaining boundary conditions to be satisfied at  $\mathscr{Y} = 0$  depend on the nature of the surface and result from the momentum balance. The two extreme cases correspond to a stress-free surface and a no-slip wall, respectively. The first of these descriptions applies at an interface where the fluid under consideration is in contact with another fluid of vanishingly small density and viscosity, the interfacial tension of the pair of fluids being large. Then, provided the intensity of the turbulence is moderate, the surface remains approximately flat because for each eddy size either the Froude number or the Weber number is low. In the absence of any surface tension gradient, the momentum balance then leads to the vanishing of the interfacial shear stress, which itself reduces (by virtue of the kinematic condition (1)) to the vanishing of the normal gradient of the tangential velocity, i.e.  $\partial(\mathbf{n} \times \mathbf{v}')/\partial\mathscr{Y} = \mathbf{0}$  at  $\mathscr{Y} = 0$ . Combining this condition with (1), one finds that only the normal component  $\boldsymbol{\omega}' \cdot \mathbf{n}$  of the vorticity fluctuation can exist at the surface, the direct consequence of this being that vortex lines are normal to the surface. Moreover the solenoidality condition  $\nabla \cdot \boldsymbol{\omega}' = 0$  implies that the normal gradient of  $\boldsymbol{\omega}' \cdot \mathbf{n}$  must also vanish at the surface. Hence the boundary conditions to be satisfied at  $\mathscr{Y} = 0$  by  $\boldsymbol{\omega}_A$  are

$$\boldsymbol{\omega}_A \times \mathbf{n} = -\boldsymbol{\omega}_\infty \times \mathbf{n}, \quad (8a)$$

$$\frac{\partial}{\partial\mathscr{Y}}(\mathbf{n} \cdot \boldsymbol{\omega}_A) = -\frac{\partial}{\partial\mathscr{Y}}(\mathbf{n} \cdot \boldsymbol{\omega}_\infty). \quad (8b)$$

In the case of a solid wall or an interface strongly contaminated by surfactants, the velocity fluctuation must satisfy a no-slip condition at  $\mathscr{Y} = 0$ , i.e.  $\mathbf{n} \times \mathbf{v}' = \mathbf{0}$ . Therefrom, it turns out that the normal component of  $\boldsymbol{\omega}'$  must vanish at  $\mathscr{Y} = 0$ , a condition implying that vortex lines are parallel to the surface. Moreover, inserting (1) into the definition of the tangential component of  $\boldsymbol{\omega}'$  shows that at  $\mathscr{Y} = 0$  the

value of this component is directly related to the normal gradient of the tangential velocity. The complete boundary condition to be satisfied by  $\omega_A$  can then be written in the compact form

$$\omega_A = -\omega_\infty + \frac{\partial}{\partial \mathcal{Y}}(\mathbf{n} \times (\mathbf{v}_\infty + \nabla\Phi + \mathbf{v}_A)). \tag{9}$$

Whatever the boundary condition at the surface, the vortical and potential velocity disturbances can be defined unambiguously by splitting the kinematic condition (1) into two boundary conditions to be satisfied separately, namely

$$\mathbf{n} \cdot \mathbf{v}_A = 0, \tag{10}$$

$$\mathbf{n} \cdot \nabla\Phi = -\mathbf{n} \cdot \mathbf{v}_\infty. \tag{11}$$

The irrotational velocity disturbance  $\nabla\Phi$  can then be determined at any time by solving (5) subject to boundary conditions (7b) and (11). Similarly, starting from the initial condition  $\omega_A = \mathbf{0}$ , the vorticity disturbance can be determined through a time-marching procedure by solving (6) subject to boundary conditions (7a), (8a, b) or (9). At each time  $t$ , one also needs to determine the vortical velocity disturbance  $\mathbf{v}_A(\mathbf{X}, t) = \nabla \times \mathbf{A}(\mathbf{X}, t)$  involved in (6) and, if necessary, in the boundary condition (9). This is achieved by solving (4) for the vector potential  $\mathbf{A}$ , subject to appropriate boundary conditions. Clearly, one must have

$$\mathbf{A} \rightarrow \mathbf{0} \quad \text{for} \quad \mathcal{Y} \rightarrow \infty. \tag{12a}$$

After some algebra, it may be shown that imposing the surface conditions

$$\mathbf{n} \times \mathbf{A} = \mathbf{0}, \quad \partial(\mathbf{n} \cdot \mathbf{A})/\partial \mathcal{Y} = 0 \tag{12b}$$

together with conditions (7a), (8a, b) for  $\omega_A$  guarantees that (10) and the stress-free condition are satisfied at  $\mathcal{Y} = 0$ . Similarly, setting the surface condition

$$\mathbf{A} = \mathbf{0} \tag{12c}$$

at  $\mathcal{Y} = 0$  together with (7a) and (9) guarantees that (10) and the no-slip condition are satisfied.

### 2.2. The RDT approach of the problem

The foregoing set of equations specifies completely the mathematical problem to be solved in order to find at any time the velocity disturbance induced by the presence of the surface. Owing to the boundary condition (11), the scalar potential  $\Phi$  may be determined independently from the vortical disturbance. This is exactly what is achieved in the HG theory, in the sense specified below. In contrast, the vortical disturbance  $\mathbf{v}_A$  is not considered at all in this theory because HG focused on the solution at short time following insertion of a flat surface (i.e. the situation depicted in figure 1b), and  $\|\mathbf{v}_A\| \rightarrow 0$  for  $t \rightarrow 0$ . Hence, in contrast to the usual RDT approaches in which the distortion of the flow consists of an imposed shear or strain whose main effect is to modify the initial large-scale vorticity field, the ‘rapid distortion’ considered in the HG theory does not affect the vorticity field at all. The distortion of the vorticity field due to the large-scale strain induced by the irrotational disturbance  $\nabla\Phi$  occurs on larger (advective) time scales and is precisely the contribution we wish to evaluate in order to determine to what extent the ‘rapid’ solution of HG is altered at large time.

Two points should now be mentioned. First, if we were able to solve the above set of equations for an arbitrary undisturbed flow field  $\mathbf{v}_\infty(\mathbf{X}, t)$ , it would be possible to

compute individual realizations of the flow field as is done in the DNS approach. As usual, the RDT theory simplifies the complete problem by using a linearized form of the momentum (or vorticity) equation, and by only taking into account statistical information on the spatial structure of the flow field  $\mathbf{v}_\infty$  through the energy spectrum. In particular, two-time correlations of the undisturbed turbulence are not specified. Hence, results of the HG theory and the present results must necessarily be interpreted in a statistical sense (to obtain one-time statistics) and cannot be used to predict individual realizations of the flow, even though the mathematical developments are performed on a single realization of  $\mathbf{v}_\infty$  (see the beginning of Appendix A). Second, as mentioned above, the purpose of the original HG theory was to study the short-time evolution of the turbulent field following the insertion of the surface (corresponding to Figure 1*b*). Hence only the specification of the spectral characteristics of the initial flow field  $\mathbf{v}_0(\mathbf{X}) = \mathbf{v}_\infty(\mathbf{X}, t=0)$  was required in this approach. Here, as we are concerned with the long-time behaviour of the flow (figure 1*c*), we need an extended interpretation of RDT (Carlotti 2001). This is why we required  $\mathbf{v}_\infty(\mathbf{X}, t)$  to be a solution of the Navier–Stokes equations at any time in the absence of the surface. Such an ‘extended’ or ‘time-marching’ RDT concept encompasses the classical ‘short-time’ RDT and has already been used by several authors in conjunction with the Eulerian kinematic simulation technique, in particular to obtain two-point correlations in a turbulent flow in the presence of a wall (Turfus & Hunt 1987; Carlotti 2002). These authors computed two-point near-wall statistics, starting from a collection of realizations of the velocity field  $\mathbf{v}_\infty(\mathbf{X}, t)$  having random phases, the amplitudes of  $\mathbf{v}_\infty$  in Fourier space being prescribed according to a given energy spectrum.

### 2.3. The spatial structure of the surface-influenced layer

Let us now come back to the governing equations derived above and to some of their consequences. From (5) and (11) we see that no explicit length scale occurs in the problem defining  $\Phi$ . However, since the boundary condition (11) involves the velocity field  $\mathbf{v}_\infty$  whose large scales are of the order of the integral length scale  $L_\infty$  characterizing the undisturbed turbulence, the irrotational disturbance  $\nabla\Phi$  can only have a significant magnitude throughout a layer whose thickness is of order  $L_\infty$  (figure 1*b, c*). Owing to boundary conditions (8) or (9), a viscous sublayer develops in time along the surface (figure 1*b*). For short times, the growth of this sublayer is governed by the linear part of (6) (first term on the left-hand side). Thus the thickness  $\delta_V$  of the viscous sublayer evolves classically as  $\delta_V(t) \sim (\nu t)^{1/2}$  at short time, i.e.  $t \ll L_\infty/u_\infty$  where  $u_\infty$  is the r.m.s. velocity characterizing the undisturbed turbulence. At larger times, i.e.  $t \gg L_\infty/u_\infty$ , the growth of the viscous sublayer saturates because of the processes associated with the nonlinear terms of (6). Hence the stationary value of  $\delta_V$  is of the order of that reached at  $t \sim L_\infty/u_\infty$ , that is  $\delta_V \sim (\nu L_\infty/u_\infty)^{1/2}$  (figure 1*c*). Measurements by Brumley & Jirka (1987) and LES results of CM indicate  $\delta_V/L_\infty \approx 2Re_\infty^{-1/2}$ , where  $Re_\infty$  is the turbulent Reynolds number defined as  $Re_\infty = 2u_\infty L_\infty/\nu$ . Note that in flows where  $Re_\infty$  is very large, typically in geophysical situations with  $Re_\infty > 10^4$ – $10^5$ , the Reynolds number  $Re_\nu = 2u_\infty \delta_V/\nu \sim Re_\infty^{1/2}$  is large enough for eddies travelling within the viscous sublayer to become unstable, especially if a no-slip condition applies at the surface. Then, the structure of this sublayer becomes more complex than depicted in figure 1(*c*), with, in particular, the development of a so-called ‘eddy surface layer’ with peculiar spectral characteristics (Hunt & Carlotti 2001). Here we are mainly interested in the dynamics of the turbulent flow in the nearly inviscid region of the surface-influenced layer, i.e. within the

so-called source layer defined approximately as  $\delta_V \leq \mathcal{Y} \leq L_\infty$  (see figure 1*b, c*). Hence, there is no upper bound in terms of the magnitude of  $Re_\infty$  on the validity of the results derived below; nevertheless, a complete description of the shear-free boundary layer would of course require a complementary study focused on the long-time dynamics of the viscous sublayer.

### 3. The validity of the Hunt–Graham theory at large time

#### 3.1. Consequences of the enstrophy balance

According to (4) we have  $\langle \omega'^2 \rangle = \langle \omega_\infty^2 \rangle + 2\langle \omega_\infty \cdot \omega_A \rangle + \langle \omega_A^2 \rangle$ , where the angle brackets denote spatial averaging in directions  $x$  and  $z$ . It is thus appropriate to define the dimensionless parameter  $\zeta$  characterizing the relative magnitude of the enstrophy disturbance as

$$\zeta = |2\langle \omega_\infty \cdot \omega_A \rangle + \langle \omega_A^2 \rangle| / \langle \omega_\infty^2 \rangle. \quad (13)$$

Within the viscous sublayer the dynamics of the flow in the presence of the surface are necessarily different from those of the undisturbed flow because  $\zeta$  is of order unity at the surface (see conditions (8)–(9)). The short-time dynamics of this viscous sublayer were recently studied by Teixeira & Belcher (2000) within the framework of RDT. In the presence of a rigid wall, inviscid RDT analyses of this sublayer in situations where the turbulent Reynolds number is so large that eddies scraping along the wall develop an instantaneous logarithmic layer have recently been carried out by Hunt & Carloti (2001) and Carloti (2002). Outside this sublayer, effects of boundary conditions (8) or (9) are negligible and the generation of the vorticity disturbance  $\omega_A$  is essentially due to the terms on the right-hand side of (6). These terms, which represent the transport, stretching and tilting of  $\omega_\infty$  by the irrotational disturbance  $\nabla\Phi$  and its gradients, were neglected in the HG analysis which can thus be considered as a zeroth-order solution with respect to  $\zeta$ . Within the source layer for which this theory was constructed,  $\zeta$  is small compared to unity for small times, i.e.  $tu_\infty/L_\infty = o(1)$ , because the characteristic time of the nonlinear processes is of order  $L_\infty/u_\infty$ . Consequently, to make some progress on the controversies discussed in the introduction, we need to clarify the conditions under which  $\zeta$  can remain small compared to unity at large time within the source layer. The simplest way by which we can obtain some information about  $\zeta$  is to determine the order of magnitude of the various terms involved in the enstrophy budget. In the present flow this budget is written, in index notation (Tennekes & Lumley 1972, p. 87),

$$\left( \frac{\partial}{\partial t} - \nu \frac{\partial^2}{\partial \mathcal{Y}^2} \right) \left\langle \frac{\omega'_i \omega'_i}{2} \right\rangle = - \frac{\partial}{\partial \mathcal{Y}} \left\langle v' \omega'_i \omega'_i \right\rangle + \left\langle \omega'_i \omega'_j \frac{\partial v'_i}{\partial x_j} \right\rangle - \nu \left\langle \frac{\partial \omega'_i}{\partial x_j} \frac{\partial \omega'_i}{\partial x_j} \right\rangle, \quad (14a)$$

where  $\omega'_i$  is the  $i$ th component of  $\omega'$ ,  $v'$  is the component of  $\mathbf{v}'$  in the direction normal to the surface and the Einstein convention on repeated indices is used.

Terms on the left-hand side of (14a) represent the time-rate-of-change and viscous diffusion of enstrophy, whereas those on the right-hand side represent transport in the direction normal to the surface, production by vortex stretching and dissipation, respectively. Let us now assume that the undisturbed flow is homogeneous in the  $\mathcal{Y}$ -direction. This is the situation for which the HG theory was elaborated, so that the estimates given below are only rigorously obtained for this case. Then the enstrophy balance governing the evolution of  $\omega_\infty$  reduces to

$$\frac{\partial}{\partial t} \left\langle \frac{\omega'_{i\infty} \omega'_{i\infty}}{2} \right\rangle = \left\langle \omega'_{i\infty} \omega'_{j\infty} \frac{\partial v'_{i\infty}}{\partial x_j} \right\rangle - \nu \left\langle \frac{\partial \omega'_{i\infty}}{\partial x_j} \frac{\partial \omega'_{i\infty}}{\partial x_j} \right\rangle. \quad (14b)$$

From the definition of the Taylor microscale  $\lambda$ , it is obvious that the stretching term in (14b) is of order  $u_\infty^3/\lambda^3$ . The detailed order-of-magnitude analysis of Tennekes & Lumley (1972, pp. 90–92) shows that the time-rate-of-change term is smaller than  $u_\infty^3/\lambda^3$  by a factor of order  $Re_\infty^{-1/2}$ . Therefrom, the least-degeneracy principle leads to the well-known conclusion that the dissipation term is necessarily of order  $u_\infty^3/\lambda^3$ .

To make apparent the source terms responsible for the enstrophy disturbance near the surface, we can rewrite the transport term in (14a) in the form  $(\partial/\partial\mathcal{Y})\langle(v_\infty + \partial\Phi/\partial\mathcal{Y})\omega_{\infty i}\omega_{\infty i}/2\rangle + \langle\mathcal{F}\rangle$  where  $\langle\mathcal{F}\rangle$  groups contributions involving  $\omega_A$ ,  $v_A$  or both (near the edge of the viscous sublayer,  $\langle\mathcal{F}\rangle$  contains in particular the residual flux of the enstrophy disturbance  $(\omega_A \cdot \omega_A)/2$  due to boundary conditions (8) or (9)). Similarly we rewrite the stretching term in the form  $\langle\omega_{\infty i}\omega_{\infty j}(\partial/\partial x_j)(v_{\infty i} + \partial\Phi/\partial x_i)\rangle + \langle\mathcal{G}\rangle$ . To evaluate the magnitude of  $\zeta$  we first need an estimate of the foregoing source terms. According to the definition of  $\zeta$ ,  $\langle\omega_i^2\rangle = O((1 \pm \zeta)u_\infty^2/\lambda^2)$ . Then we introduce the estimates appropriate within the source layer, i.e.  $\partial/\partial\mathcal{Y} = O(1/\mathcal{Y})$  and  $|v_\infty + \partial\Phi/\partial\mathcal{Y}| = O(u_\infty(\mathcal{Y}/L_\infty)^{1/3})$  (see Appendix A). We also take into account the fact that the correlation between velocity and vorticity fluctuations must be weighted by a ratio  $\lambda/L_\infty$  because the characteristic wavenumber of velocity (resp. vorticity) fluctuations is  $L_\infty^{-1}$  (resp.  $\lambda^{-1}$ ), resulting in a weak spectral overlap (Tennekes & Lumley 1972, p. 81). From these estimates we conclude that

$$\left| \frac{\partial}{\partial\mathcal{Y}} \left\langle \left( v_\infty + \frac{\partial\Phi}{\partial\mathcal{Y}} \right) \frac{\omega_{\infty i}\omega_{\infty i}}{2} \right\rangle \right| \sim \left( \frac{u_\infty}{\lambda} \right)^3 \left( \frac{\lambda}{L_\infty} \right)^2 \left( \frac{L_\infty}{\mathcal{Y}} \right)^{2/3} \sim Re_\infty^{-1} \left( \frac{u_\infty}{\lambda} \right)^3 \left( \frac{L_\infty}{\mathcal{Y}} \right)^{2/3}, \quad (15a)$$

where the last equality is obtained by using the well-known estimate  $\lambda/L_\infty = O(Re_\infty^{-1/2})$  (note that this estimate still holds within the source layer, as shown at the end of Appendix A). To estimate the term  $\langle\omega_{\infty i}\omega_{\infty j}(\partial/\partial x_j)(v_{\infty i} + \partial\Phi/\partial x_i)\rangle$  in (14a) we need to know the order of magnitude of velocity gradients within the source layer. Their variance is calculated in Appendix A using the HG expression for the velocity potential  $\Phi$ ; (A 7) allows us to conclude that the r.m.s. value of these velocity gradients is of order  $u_\infty/\lambda(1 \pm (k_K\mathcal{Y})^{-4/3})^{1/2}$  instead of being of order  $u_\infty/\lambda$  in the free stream,  $k_K$  being the Kolmogorov wavenumber associated with small-scale dissipative eddies (a precise definition of  $k_K$  is given in Appendix A, above (A 5)). In the limit  $Re_\infty \rightarrow \infty$ ,  $k_K\mathcal{Y}$  is large within the source layer because  $k_K L_\infty = O(Re_\infty^{3/4})$  (Monin & Yaglom 1975, p. 349). Consequently the correction induced by the irrotational disturbance is small. This was to be expected because, at a given  $\mathcal{Y}$ , only ‘large’ eddies with a tangential wavenumber smaller than  $1/\mathcal{Y}$  are affected by the surface (see (A 2)), whereas the main contribution to the velocity gradients comes from small-scale eddies. Using the estimate  $k_K L_\infty = O(Re_\infty^{3/4})$ , the magnitude of the correction experienced by the velocity gradients within the source layer is found to be of order  $u_\infty/\lambda Re_\infty^{-1}(L_\infty/\mathcal{Y})^{4/3}$ . Therefore, given the relative distance  $\mathcal{Y}/L_\infty$  from the surface, the larger the turbulent Reynolds number the smaller the correction because of the increasing gap between large- and small-scale eddies. From the foregoing result we conclude that an upper bound for the source term  $\langle\omega'_{\infty i}\omega'_{\infty j}(\partial/\partial x_j)(v'_{\infty i} + \partial\Phi/\partial x_i)\rangle$  is

$$\left| \left\langle \omega_{\infty i}\omega_{\infty j} \frac{\partial}{\partial x_j} \left( v_{\infty i} + \frac{\partial\Phi}{\partial x_i} \right) \right\rangle \right| = O \left( \left( \frac{u_\infty}{\lambda} \right)^3 \left( 1 \pm Re_\infty^{-1} \left( \frac{L_\infty}{\mathcal{Y}} \right)^{4/3} \right) \right). \quad (15b)$$

Comparing (15a) with (15b) reveals that the surface-induced correction to the stretching term is larger than the transport term by a factor  $(L_\infty/\mathcal{Y})^{2/3}$ . Consequently, this correction is the main source for the enstrophy disturbance within the source

layer. To estimate the dissipation term we use the fact that the characteristic length scale of vorticity gradients is the Kolmogorov microscale  $\eta_K$  (Tennekes & Lumley 1972, p. 92). This yields

$$\begin{aligned} \nu \left| \left\langle \frac{\partial \omega'_i}{\partial x_j} \frac{\partial \omega'_i}{\partial x_j} \right\rangle \right| &\sim \left( (1 \pm \zeta) \frac{\nu}{\eta_K^2} \left( \frac{u_\infty}{\lambda} \right)^2 \right) \sim \left( (1 \pm \zeta) Re_\infty^{-1} \frac{\lambda L_\infty}{\eta_K^2} \left( \frac{u_\infty}{\lambda} \right)^3 \right) \\ &\sim \left( (1 \pm \zeta) \left( \frac{u_\infty}{\lambda} \right)^3 \right), \end{aligned} \quad (15c)$$

where the last equality is obtained by making use of the relations  $\lambda/L_\infty = O(Re_\infty^{-1/2})$  and  $\eta_K/L_\infty = O(Re_\infty^{-3/4})$ . Finally we note that the time-rate-of-change term in (14a) is

$$\frac{\partial}{\partial t} \left\langle \frac{\omega'_i \omega'_i}{2} \right\rangle \sim \left( (1 \pm \zeta) Re_\infty^{-1/2} \left( \frac{u_\infty}{\lambda} \right)^3 \right), \quad (15d)$$

whereas the viscous contribution is smaller than the latter term by a factor  $Re_\infty^{-1}$ . When a statistical equilibrium is reached, the source terms in (14a) are balanced either by the nonlinear terms  $\langle \mathcal{F} \rangle$  and  $\langle \mathcal{G} \rangle$  or by dissipation. It is difficult to determine precisely the order of magnitude of  $\langle \mathcal{F} \rangle$  and  $\langle \mathcal{G} \rangle$  because these terms involve products of quantities whose degree of correlation is *a priori* unknown (particularly because we do not know to what extent the spatial scales of the vorticity disturbance  $\omega_A$  overlap those of the undisturbed velocity field  $\mathbf{v}_\infty$ ). However, since all contributions in  $\langle \mathcal{F} \rangle$  and  $\langle \mathcal{G} \rangle$  involve either  $\omega_A$  or the associated vortical velocity disturbance  $\mathbf{v}_A$  or both, we necessarily have  $\langle \mathcal{F} \rangle = \langle \mathcal{G} \rangle = 0$  for  $\zeta = 0$ . More precisely,  $\langle \mathcal{G} \rangle$  involves for instance terms like  $\omega_{Ai} \omega_{oj} \partial v_{\infty i} / \partial x_j$  or  $\omega_{Ai} \omega_{Aj} \partial v_{\infty i} / \partial x_j$ . Using the Schwarz inequality and (13), it turns out that the order of magnitude of these terms cannot exceed  $\zeta u_\infty^3 / \lambda^3$ , which leads us to conclude that the Taylor expansion of  $\langle \mathcal{F} \rangle$  and  $\langle \mathcal{G} \rangle$  with respect to  $\zeta$  begins with a term linearly proportional to  $\zeta$ . We can now insert the above estimate of  $\langle \mathcal{F} \rangle$  and  $\langle \mathcal{G} \rangle$  and the results (15a–d) into (14a). Moreover, we know that terms associated with the undisturbed flow field (i.e. terms independent of  $\zeta$  and  $\mathcal{Y}$  in (15b–d)) balance exactly because they satisfy the undisturbed enstrophy balance (14b). Thus, it turns out that the term proportional to  $Re_\infty^{-1} (L_\infty / \mathcal{Y})^{4/3}$  in (15b) must be balanced by a term of order  $\zeta u_\infty^3 / \lambda^3$ , due either to viscous dissipation or to the nonlinear contributions  $\langle \mathcal{F} \rangle$  and  $\langle \mathcal{G} \rangle$ . This yields

$$\zeta = O \left( Re_\infty^{-1} \left( \frac{L_\infty}{\mathcal{Y}} \right)^{4/3} \right). \quad (16)$$

Equation (16) is the central result of the present analysis. It shows that within the source layer, the straining associated with the distortion of large eddies by the surface is much weaker than  $u_\infty / \lambda$  and produces an enstrophy disturbance whose relative order of magnitude at long time ranges from  $\zeta = O(Re_\infty^{-1})$  for  $\mathcal{Y} / L_\infty = O(1)$  to  $\zeta = O(Re_\infty^{-1/3})$  for  $\mathcal{Y} \approx \delta_V$ , i.e.  $\mathcal{Y} / L_\infty = O(Re_\infty^{-1/2})$  (see figure 1c). It must be kept in mind that this estimate provides only an upper bound of the enstrophy disturbance. Nevertheless the crucial point is that  $\zeta$  remains small throughout the source layer. Consequently our main result is that, provided the turbulent Reynolds number is large enough, the distortion of the undisturbed vorticity field by the irrotational disturbance  $\nabla \Phi$  is only a secondary effect at all times in this flow, which allows us to conclude that the HG description of the source layer is valid even at large time. Obviously, estimates (15a, b) are specific to the source layer (see the assumptions used in Appendix A), so that the result (16) does not hold within the viscous sublayer.

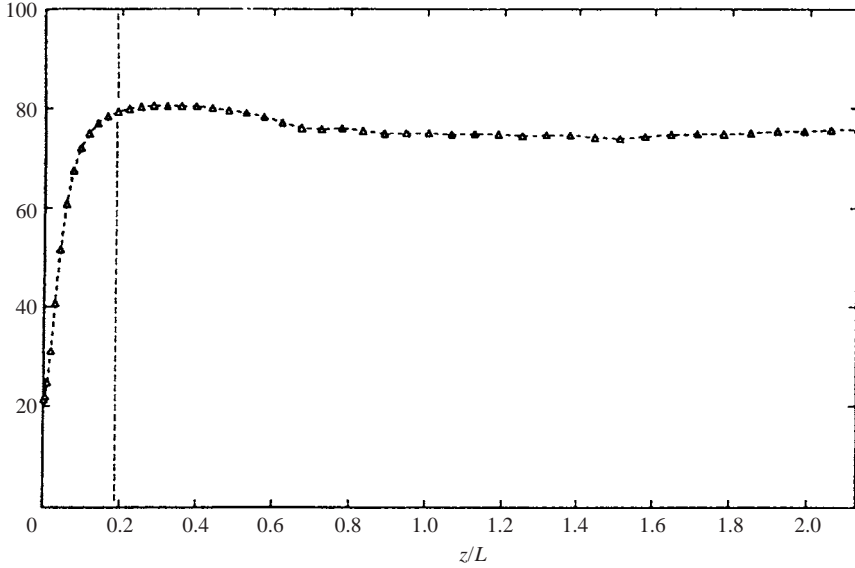


FIGURE 2. The enstrophy profile near the shear-free surface in the time-evolving DNS of Walker *et al.* (1996).  $Re_\infty \approx 65$ ; enstrophy is normalized by  $(\varepsilon_\infty/K_\infty)^2$  ( $\varepsilon_\infty$  and  $K_\infty$  are the free-stream dissipation rate and kinetic energy, respectively). The vertical line indicates approximately the edge of the viscous sublayer.

Note however that our estimate of  $\langle \mathcal{F} \rangle$  and  $\langle \mathcal{G} \rangle$  (which were found to be of order  $\zeta u_\infty^3/\lambda^3$ ) is consistent with the fact that at the top of the viscous sublayer (where  $\zeta$  is of order unity because of boundary conditions (8)–(9)), these terms are of order  $u_\infty^3/\lambda^3$ , i.e. of the same order of magnitude as the dominant terms of (14b).

The prediction (16) can be checked by comparison with the numerical results of WLGR who examined the evolution of the enstrophy throughout the flow (figure 2, reprinted from figure 6b of the original paper). In this simulation,  $Re_\infty$  is about 65 so that (16) yields  $\zeta \approx 0.1$  at the position  $\mathcal{Y}/L_\infty = 2.0 Re_\infty^{-1/2}$  corresponding to the outer edge of the viscous sublayer. At this location ( $z/L \approx 0.2$  in WLGR's notation), the results exhibit a broad maximum of the enstrophy that is larger than the free-stream value by about 9%, in good agreement with our estimate. Interesting information can also be obtained by considering (14a) separately for each component of  $\langle \omega_i'^2 \rangle$  (no summation on  $i$ ). More precisely, we may repeat the analysis leading to (15b) for each component of  $\langle \omega_i'^2 \rangle$ , using results from (A 7). This equation shows that  $\langle (\partial u'/\partial \mathcal{Y})^2 \rangle$  and  $\langle (\partial w'/\partial \mathcal{Y})^2 \rangle$  increase in the source layer as  $\mathcal{Y}/L_\infty \rightarrow 0$  whereas  $\langle (\partial v'/\partial x)^2 \rangle$  and  $\langle (\partial v'/\partial z)^2 \rangle$  decrease, a tendency qualitatively confirmed by the results of Shen *et al.* (1999) (according to (A 7), the other five components of the r.m.s. velocity gradient are left unaffected by the surface). Using these results in the evaluation of the vortex stretching term involved in the balance equation of  $\langle \omega_x'^2 \rangle$  and  $\langle \omega_z'^2 \rangle$  (resp.  $\langle \omega_y'^2 \rangle$ ), we find that this term increases (resp. decreases) within the source layer as  $\mathcal{Y}/L_\infty \rightarrow 0$ . Hence we can conclude that the magnitude of the tangential components  $\omega_x'$  and  $\omega_z'$  increases as the surface is approached, while that of the normal component decreases; this conclusion is also supported by the results of WLGR.

### 3.2. Discussion

At this point several comments are in order. First, it is clear from (16) that the lower the Reynolds number, the larger the departure of the actual velocity field from

the HG predictions. The largest differences are found near the outer edge of the viscous sublayer and these differences are larger by a factor of order  $Re_\infty^{1/6}$  than the viscous corrections, which are of order  $Re_\infty^{-1/2}$ . For sufficiently small values of  $Re_\infty$ , other low-Reynolds-number effects associated with the boundary conditions (8) or (9) affect the surface-influenced layer because  $\delta_v$  is a substantial percentage of  $L_\infty$ . These effects are more noticeable in the case of a solid wall than in that of a shear-free surface because the tangential velocity fluctuations must then return to zero (Teixeira & Belcher 2000). For instance the HG theory predicts that the turbulent kinetic energy increases towards the surface for  $\mathscr{Y}/L_\infty \leq 0.27$ . This effect will certainly not be observed if  $\delta_v/L_\infty$  is larger than 0.15–0.20. As was pointed out by HG, there is little doubt that this is why the low-Reynolds-number experiments of Uzkan & Reynolds (1967) did not exhibit a maximum of the tangential fluctuations close to the wall; the results of Aronson *et al.* (1997) are also probably affected by this effect, even though the corresponding value of  $Re_\infty$  is about four times larger than in the former experiment. These remarks suggest that DNS predictions obtained with low values of  $Re_\infty$  must be interpreted with care. Clearly there is no reason to expect that such DNS results will agree with the HG theory in the region of maximum influence of the surface, i.e. for small values of  $\mathscr{Y}/L_\infty$ . Moreover, since high-Reynolds-number experimental and LES results agree with HG predictions, we believe that some of the conclusions that have been drawn from low-Reynolds-number DNS for modelling the influence of a flat surface on terms like dissipation and pressure–strain correlation (Perot & Moin 1995*b*) should be restricted to low Reynolds numbers.

Second, we observe that our estimate of nonlinear effects differs markedly from the correction proposed by Hunt (1984), according to which the tangential velocity variances increase near the surface by  $(\Delta u)^2 = O(u_\infty^2(L_\infty/\mathscr{Y})^{1/2})$  owing to the extra vorticity generated by large-scale strain. We find a much smaller amplification, since, for  $\mathscr{Y}/L_\infty = O(Re_\infty^{-1/2})$ , (16) predicts  $(\Delta u)^2 = O(u_\infty^2 Re_\infty^{-1/3})$  instead of  $(\Delta u)^2 = O(u_\infty^2 Re_\infty^{1/4})$  based on Hunt’s estimate. Hunt derived his correction on the basis of an analogy with results obtained by Durbin (1981) in a study of turbulence amplification near the front stagnation point of a sphere. This analogy is revisited in Appendix C where we show that an important mathematical constraint required for the applicability of Durbin’s results is not satisfied in the surface-influenced layer. As far as we are aware, the only observations to date that support Hunt’s nonlinear correction are those of Hannoun *et al.* (1988) and Kit *et al.* (1997) obtained in a stirred-grid tank in the presence of a sharp density interface. However, these authors noticed the existence of interfacial waves in the flow, and the corresponding velocity spectra suggest that a significant part of the increase of the horizontal fluctuations near the interface is due to these waves which feed the low-wavenumber components, whereas on the grounds of Hunt’s correction one would expect an enhancement of significantly smaller eddies. Moreover, Hannoun *et al.* and Kit *et al.* normalized the results they obtained at a distance  $\mathscr{Y}$  from the interface using the r.m.s. velocity fluctuation  $u_H(\mathscr{Y})$  measured at the same location in a homogeneous fluid. In contrast, the results of Brumley & Jirka (1987) (basically obtained in the same type of device and in the same range of  $Re_\infty$ ) and those of Calmet & Magnaudet (2003) were normalized using the ‘free-stream’ intensity  $u$  corresponding to  $\mathscr{Y} = L_\infty$  and did not exhibit any over-amplification of the horizontal fluctuations compared to the original HG theory. According to Kit *et al.*,  $u_H^2(\mathscr{Y} = 0)/u^2$  is about 0.75 in these experiments, so that most of the over-amplification noticed by the aforementioned authors disappears if their results are renormalized using  $u$  instead of  $u_H$ .

From the above remarks it seems that the agreement between the results of Hannoun *et al.* and Kit *et al.* and Hunt's correction is most likely fortuitous, and the conclusions of the analysis carried out in Appendix C suggest that this correction itself is questionable. Nevertheless there is no doubt that the stretching of small-scale turbulence by large-scale eddies always tends to amplify tangential fluctuations near the surface. As our analysis is global because it does not take into account the distribution of length scales of small eddies, it is probable that a certain subrange of eddies undergoes an amplification larger than predicted by (16) and thus closer to RDT predictions. However, the crucial difference between inviscid RDT predictions and our analysis is that we take into account the moderating effect of viscous dissipation. Hence, even though (16) probably underpredicts the amplification of certain small-scale eddies, what our analysis shows is that when the entire spectrum is considered, dissipation limits the effects of the nonlinear amplification mechanism to the level specified by (16).

### 3.3. Governing equations and pressure fluctuation within the source layer

Using the conclusions of §3.1 we now consider the flow field in the source layer in the limit  $Re_\infty \rightarrow \infty$ . Having shown that the vorticity disturbance  $\boldsymbol{\omega}_A$  and hence the vortical velocity correction  $\mathbf{v}_A$  are negligibly small whatever  $t$  in this limit, we shall neglect from now on terms of order  $\zeta$ . Hence the leading-order velocity field in the source layer is merely

$$\mathbf{v}'(\mathbf{X}, t) \approx \mathbf{v}_\infty(\mathbf{X}, t) + \nabla\Phi(\mathbf{X}, t). \quad (17)$$

The Navier–Stokes equations corresponding to the velocity field (17) are

$$\frac{\partial}{\partial t}(\mathbf{v}_\infty + \nabla\Phi) + \frac{1}{2}\nabla(\mathbf{v}_\infty + \nabla\Phi)^2 + \boldsymbol{\omega}_\infty \times (\mathbf{v}_\infty + \nabla\Phi) = -\frac{1}{\rho}\nabla(p_\infty + \mathcal{P}') + \nu\nabla^2\mathbf{v}_\infty, \quad (18)$$

where  $\rho$  denotes the fluid density,  $p' = p_\infty + \mathcal{P}'$  is the total pressure fluctuation and use has been made of the fact that viscous stresses induced by the irrotational disturbance  $\nabla\Phi$  do not produce any momentum flux, since  $\nabla^2(\nabla\Phi) = -\nabla \times (\nabla \times (\nabla\Phi)) = \mathbf{0}$ . As we can see in (6), negligible values of  $\boldsymbol{\omega}_A$  in the source layer correspond to negligible values of the term  $\nabla\Phi \cdot \nabla\boldsymbol{\omega}_\infty - \boldsymbol{\omega}_\infty \cdot \nabla(\nabla\Phi) = \nabla \times [\boldsymbol{\omega}_\infty \times \nabla\Phi]$ . Consequently, the leading part of  $\boldsymbol{\omega}_\infty \times \nabla\Phi$  is associated with a scalar potential  $\Psi$ , so that we may write  $\boldsymbol{\omega}_\infty \times \nabla\Phi = \nabla\Psi + O(\zeta u_\infty^2/\lambda)$ . Then, subtracting the momentum equation governing the unperturbed field  $\mathbf{v}_\infty$  from (18), in which we neglect the above contribution of order  $\zeta u_\infty^2/\lambda$ , yields a relation giving the leading-order pressure gradient  $\nabla\mathcal{P}'$  induced by the presence of the surface. This relation may be integrated once, allowing us to write a Bernoulli-like integral giving  $\mathcal{P}'$  in the form

$$\mathcal{P}'(\mathbf{X}, t) = -\rho \left\{ \frac{\partial\Phi}{\partial t} + \frac{1}{2}(\nabla\Phi)^2 + \mathbf{v}_\infty \cdot \nabla\Phi + \Psi \right\}(\mathbf{X}, t) + \rho \left\langle \frac{1}{2}(\nabla\Phi)^2 + \mathbf{v}_\infty \cdot \nabla\Phi + \Psi \right\rangle(\mathcal{Y}, t). \quad (19)$$

The term within angle brackets on the right-hand side accounts for the variation of the mean pressure in the direction normal to the surface ((19) does not involve any additive constant because  $\mathcal{P}'$  must vanish for  $\mathcal{Y} \rightarrow \infty$ ).

Equations (17), (19), (5), (7b) and (11) supplemented by the Navier–Stokes equations governing the undisturbed field  $(\mathbf{v}_\infty, p_\infty)$  determine completely the leading-order solution describing the inviscid influence of the surface on the pre-existing turbulence. Equations (18–19) emphasize the fact that, up to terms of order  $\zeta$ , the velocity field (17) is a solution of the full Navier–Stokes equations, i.e. momentum equations with a

nonlinear term and a viscous term. This is not widely recognized since several authors tend to oppose the ‘kinematic’ nature of the HG solution to the ‘dynamic’ nature of Navier–Stokes solutions. What is kinematic in the HG solution is the boundary condition (1) being taken into account, and a crucial consequence of this boundary condition is that no vorticity is added to the flow at leading order. As shown by (18)–(19), this by no means implies that this leading-order solution is equivalent to neglecting all nonlinearities and viscous effects in the governing equations. Bearing this crucial point in mind, transport equations for the Reynolds stress tensor  $\langle v'_i v'_j \rangle$  corresponding to the velocity field (17) can be formed by multiplying the  $i$ th and  $j$ th components of (18) by the appropriate component of (17) and averaging in directions of homogeneity. In the resulting equations, we maintain the simplifying assumptions selected for the analysis presented in § 3.1 and consider that viscous contributions are negligible within the source layer. This allows us to write the equations governing the diagonal components  $\langle v'_i v'_i \rangle$  (no summation on  $i$ ) in the form

$$\frac{\partial \langle v'_i v'_i \rangle}{\partial t} = -\epsilon_{ii} + \frac{2}{\rho} \langle p' s'_{ii} \rangle - \frac{\partial}{\partial \mathcal{Y}} \left[ \langle v'_i v'_i v' \rangle + \frac{2}{\rho} \langle p' v' \rangle \delta_{i2} \right], \quad (20)$$

where  $s'_{ii} = \partial v'_i / \partial x_i$  (resp.  $\epsilon_{ii} = \nu \langle (\partial v'_i / \partial x_j)^2 \rangle$  with summation on  $j$ ) is the diagonal component of the strain-rate (resp. pseudo-dissipation) tensor in the  $i$ th direction and  $\delta_{ij}$  is the Kronecker tensor.

#### 4. Intercomponent energy transfer

##### 4.1. The instantaneous effect of boundary insertion

To discuss the implications of (20) we have to consider separately the singular situation corresponding to  $t = 0$  (illustrated in figure 1a) and the evolution at subsequent times. At  $t = 0$ , the surface is suddenly inserted in the flow and this forces  $\partial \langle v'^2 \rangle / \partial t$  to take an infinite negative value. Owing to the term  $-\rho \partial \Phi / \partial t$  in (19), the pressure fluctuation also takes infinite values and  $\partial \langle v'^2 \rangle / \partial t$  is merely balanced by the two terms of (20) (with  $i = 2$ ) involving the pressure fluctuation. These two terms are evaluated in Appendix B where we show that they are both negative. Consequently, as one expects intuitively, the blocking effect of the surface produces an initial energy transfer from the normal energy component to the tangential ones, i.e. the pressure–strain correlation  $\phi_{22} = (2/\rho) \langle p' s'_{22} \rangle$  is negative. However, the fact that the pressure–diffusion flux  $-\partial \langle (p'/\rho) v' \rangle / \partial \mathcal{Y}$  is non-zero also implies that there is a net variation of the averaged turbulent kinetic energy per unit mass  $K = \langle \mathcal{K} \rangle$ , where  $\mathcal{K} = \frac{1}{2} \sum_{i=1}^3 v_i'^2$  is the instantaneous turbulent energy. In this case, the budget of  $K$  reduces approximately to

$$\left. \frac{\partial K}{\partial t} \right|_{t=0} \approx -\frac{1}{\rho} \frac{\partial}{\partial \mathcal{Y}} \langle p' v' \rangle. \quad (21)$$

Using the fact that  $K = \frac{3}{2} u_\infty^2$  everywhere for  $t < 0$  if the undisturbed turbulence is homogeneous and isotropic, integration of (21) yields

$$K(\mathcal{Y}, t = 0^+) = \frac{3}{2} u_\infty^2 - \frac{1}{\rho} \int_{t=0^-}^{t=0^+} \frac{\partial}{\partial \mathcal{Y}} \langle p' v' \rangle(\mathcal{Y}, t) dt. \quad (22)$$

According to (B 5), the right-hand side of (22) vanishes for  $\mathcal{Y} = 0$ , indicating that there is no change of  $K$  at the surface. Since the time integral of the pressure–diffusion flux also vanishes in the limit  $\mathcal{Y}/L_\infty \rightarrow \infty$  and is negative for finite values of  $\mathcal{Y}/L_\infty$ ,

a minimum of  $K$  occurs within the source region. The net loss of  $K$  in the flow domain is due to the fact that the time integral of  $\langle p'v' \rangle(0, t)$  between  $t=0^-$  and  $t=0^+$  is positive. This explains why a minimum of  $K$  was found at  $\mathscr{Y}/L_\infty \approx 0.27$  by HG. To conclude, this analysis confirms that the sudden insertion of the surface produces an intercomponent energy transfer by which the anisotropy of the initial turbulence becomes non-zero; however, this is not a purely redistributive process because the pressure–diffusion flux produces a net decrease of the turbulent energy in the surface-influenced region. Note that this analysis describes the ideal case where the surface is instantaneously inserted at the top of the whole flow domain. In practice, especially in wind-tunnel experiments like those reviewed in the introduction, the surface has a finite length, so that there is a leading-edge effect which by virtue of the Taylor hypothesis may be interpreted as a non-instantaneous effect of boundary insertion. This effect modifies the velocity potential  $\Phi$  near the leading edge in the way described by HG.

#### 4.2. Freely evolving turbulence

We now turn to the following stages corresponding to  $t > 0$  and consider first the situation where turbulence decays freely in time. There is no longer a singularity in the solution and we examine (20) in the limit  $\mathscr{Y}/L_\infty \rightarrow 0$ ,  $k_K \mathscr{Y} \rightarrow \infty$  corresponding to the part of the source layer closest to the surface. In this limit, the behaviour of the three r.m.s. velocities is known from (A 9) and (A 13) and the components of the pseudo-dissipation tensor  $\epsilon_{ij}$  can be deduced from (A 7). This equation also shows that the surface-induced corrections to  $\epsilon_{ii}$  are of order  $\epsilon_\infty Re_\infty^{-1} (L_\infty/\mathscr{Y})^{4/3}$ , where  $\epsilon_\infty$  is the dissipation rate in the free stream; consequently these corrections provide a contribution of order  $\epsilon_\infty Re_\infty^{-1/3}$  to (20) for  $\mathscr{Y}/L_\infty = O(Re_\infty^{-1/2})$ . To evaluate the time derivative of  $\langle v'_i v'_i \rangle$  for  $i \neq 2$  we start with (A 13) and note that the time derivative of terms proportional to  $\epsilon_\infty^{2/3} \mathscr{Y}^{2/3}$  in (A 13) is of order  $\epsilon_\infty (\mathscr{Y}/L_\infty)^{2/3}$ , thus also providing a contribution of order  $\epsilon_\infty Re_\infty^{-1/3}$  to (20) for  $\mathscr{Y}/L_\infty = O(Re_\infty^{-1/2})$ . The time derivative of the leading-order term  $\frac{3}{2} u_\infty^2$  in (A 13) is obtained by using the kinetic energy balance of the free-stream turbulence, namely

$$\frac{3}{2} \frac{du_\infty^2}{dt} = -\epsilon_\infty. \quad (23)$$

Collecting all this information allows us to approximate the Reynolds stress budget (20) for  $\mathscr{Y}/L_\infty = O(Re_\infty^{-1/2})$  as

$$2 \left\langle \frac{p'}{\rho} s'_{ii} \right\rangle - \frac{\partial}{\partial \mathscr{Y}} \langle v'_i v'_i v' \rangle \approx -\frac{1}{3} \epsilon_\infty + O(\epsilon_\infty Re_\infty^{-1/3}) \quad \text{for } i \neq 2, \quad (24)$$

$$2 \left\langle \frac{p'}{\rho} s'_{22} \right\rangle - \frac{\partial}{\partial \mathscr{Y}} \left[ \langle v'^3 \rangle + 2 \left\langle \frac{p'}{\rho} v' \right\rangle \right] \approx \frac{2}{3} \epsilon_\infty + O(\epsilon_\infty Re_\infty^{-1/3}) \quad \text{for } i = 2. \quad (25)$$

Since the pressure–strain tensor is traceless, adding (24) and (25) reveals that the transport term in the turbulent kinetic energy balance is of order  $\epsilon_\infty Re_\infty^{-1/3}$ . Assuming that none of the turbulent fluxes  $\langle v'_i v'_i v' \rangle$  can exceed this order of magnitude (a statement confirmed by the plots of WLGR), (25) implies that the pressure–strain correlation  $\phi_{22}$  is positive for large enough values of  $Re_\infty$ . More generally, the above estimates show that  $\phi_{22}$  is positive throughout the source layer, increasing from negligible values for  $\mathscr{Y}/L_\infty = O(1)$  to  $\frac{2}{3} \epsilon_\infty$  near the edge of the viscous sublayer. Thus energy is now transferred from the (largest) tangential energy components towards the (smallest) normal one, indicating that the intercomponent transfer is dominated by the isotropization mechanism generally observed far from boundaries. This happens

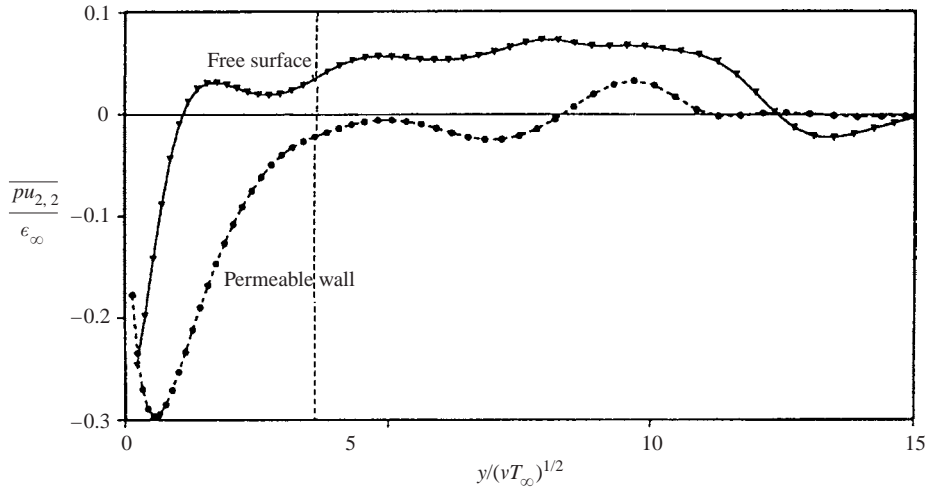


FIGURE 3. The pressure–strain correlation  $\phi_{22}$  in the time-evolving DNS of Perot & Moin (1995*a*).  $Re_\infty \approx 24$ . The vertical line indicates approximately the edge of the viscous sublayer.

because of two complementary features of the velocity variances resulting in a traceless process. First, there is a positive imbalance between the time-rate-of-change of  $\langle v'^2 \rangle$  (that vanishes at the surface) and the corresponding dissipation component  $\epsilon_{22}$ . Second, the time-rate-of-change of the tangential components  $\langle v_i'^2 \rangle$  exceeds  $\epsilon_{ii}$  because  $\langle v_i'^2 \rangle(\mathcal{A}=0, t) = 3u_\infty(t)^2/2$ , resulting in a negative imbalance. Note that there is no contradiction between the fact that the tangential r.m.s. velocities are larger than  $u_\infty$  near the surface at any time (because of the initial condition provided by the sudden insertion of the surface), and the existence of an energy transfer from these tangential components towards the normal component for  $t > 0$ . Note also that this prediction does not depend on the nature of the surface since boundary conditions (8) or (9) have not been invoked in the derivation. Confirmation that  $\phi_{22}$  takes positive values in the source layer can be found in figure 14 of PM and in figure 10 of WLGR, even though low-Reynolds-number effects reduce its magnitude significantly in these DNS results.

It must also be stressed that the foregoing results do not conflict with the findings of PM. In their simulations, the relative thickness  $\delta_V/L_\infty$  of the viscous sublayer lay between 0.25 and 0.4 approximately, depending on the Reynolds number of the simulation, and most of their discussion focused on this thick sublayer where the largest values of the pressure–strain correlation occur. There, the velocity disturbance produced by the surface is much larger in the case of a solid wall or a permeable membrane than in that of a free surface, and this led PM consistently to conclude that the strength of the pressure–strain correlation is governed by viscous processes rather than by the blocking effect. What is surprising is that PM did not comment on their results concerning the outer part of the surface-influenced region, whereas these results provide evidence of the major role played by the blocking effect outside the viscous sublayer. For instance their figure 14 (reprinted here as figure 3) compares the evolution of  $\phi_{22}$  for a shear-free surface and a permeable membrane. While these results show that  $\phi_{22}$  is clearly positive outside the viscous sublayer in the former case, they reveal near-zero values of  $\phi_{22}$  in the latter one, a trend consistent with the absence of blocking in the presence of a permeable membrane.

## 4.3. Spatially decaying turbulence

The second canonical situation of major interest for understanding how the presence of the surface affects the intercomponent energy transfer is when the undisturbed turbulence is statistically stationary and decays spatially along the direction normal to the surface, while being locally isotropic. The undisturbed flow is then governed by a balance between dissipation and turbulent transport in the  $\mathcal{Y}$ -direction, namely

$$0 = -\epsilon_{\infty}(\mathcal{Y}) - \frac{d}{d\mathcal{Y}} \left[ \langle \mathcal{K} v' \rangle_{\infty}(\mathcal{Y}) + \frac{1}{\rho} \langle p' v' \rangle_{\infty}(\mathcal{Y}) \right], \quad (26)$$

where the subscript  $\infty$  refers now to undisturbed quantities varying with  $\mathcal{Y}$  rather than to ‘free-stream’ quantities. The prototype of such turbulence (sometimes referred to as ‘purely diffusive’ turbulence) is that produced by oscillating vertically a grid at the bottom of a tank partially filled with water (see e.g. Brumley & Jirka 1987; Hannoun *et al.* 1988; Kit *et al.* 1997). Other inhomogeneous steady flows in which production by the mean shear only plays a secondary role can also probably be described with similar arguments, especially the surface region of high-Reynolds-number open-channel flow. The distortion produced by a flat surface to incoming turbulence governed by (26) is much more complex to analyse than the freely evolving case for two reasons. First, the inhomogeneity induced by the surface is superimposed on a pre-existing inhomogeneity, the presence of which greatly complicates the theoretical treatment in spectral space. This is why the mathematical extension of the HG theory to inhomogeneous turbulence is still to be done. Nevertheless, the inhomogeneity of the undisturbed flow is generally weak in the sense that relative variations of characteristic quantities like the r.m.s. velocity  $u_{\infty}$  or the dissipation  $\epsilon_{\infty}$  over one integral length scale are fairly small (typically 10% in stirred-grid experiments according to the results of Brumley & Jirka (1987)), suggesting that the main predictions of the HG theory certainly remain applicable. Second, the intercomponent energy transfer in the source layer is now governed by the near-surface behaviour of turbulent transport terms. For instance, the Reynolds stress budget in each tangential direction may be written in the form

$$\phi_{ii}(\mathcal{Y}) = \epsilon_{ii}(\mathcal{Y}) + \frac{d}{d\mathcal{Y}} \langle v'_i v'_i v' \rangle(\mathcal{Y}) \quad \text{for } i \neq 2, \quad (27)$$

where  $\phi_{ii} = 2\langle (p'/\rho)s'_{ii} \rangle$ . Hence, assuming that at leading order dissipation in the source layer remains unaffected by the surface as it is in the freely evolving case, we see that the tangential components of the pressure–strain tensor are positive or negative, depending on  $-d\langle v_i'^2 v' \rangle/d\mathcal{Y}$  being smaller or larger than  $\frac{2}{3}\epsilon_{\infty}$ . Consequently, predicting the sign of the pressure–strain terms in the surface-influenced layer requires a realistic model of third-order moments to be introduced. This is the major difficulty of the problem.

To overcome this difficulty we construct a crude near-surface model of third-order moments based on simple physical arguments. Clearly the normal motions that are most efficient for producing a net transport of the turbulent energy  $v_i'^2$  (no summation on  $i$ ) are the large-scale events characterized by a strong asymmetry (Nagano & Tagawa 1988, 1990). We can reasonably assume that the efficiency of these motions in the turbulent transport process is proportional to the skewness factor  $S(v_{\infty}) = \langle v_{\infty}^3 \rangle / \langle v_{\infty}^2 \rangle^{3/2}$  characterizing the undisturbed velocity component normal to the surface. In the part of the source layer such that  $\mathcal{Y}/L_{\infty} \ll 1$ , these large-scale motions are associated with wavenumbers much smaller than  $1/\mathcal{Y}$ . A Taylor expansion of the corresponding transport velocity  $v_s(\mathcal{Y})$  (whose average is defined as

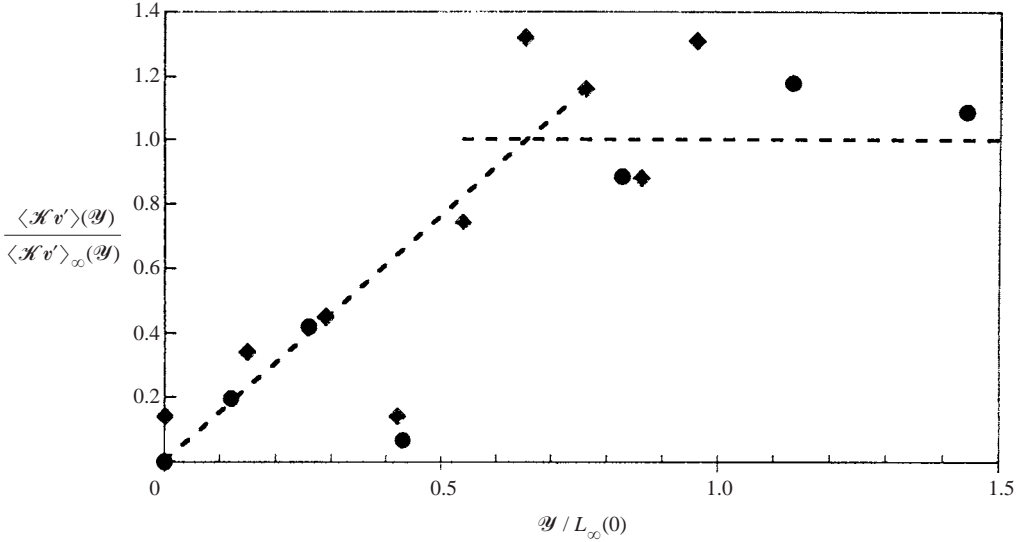


FIGURE 4. The turbulent flux  $-\langle \mathcal{H} v' \rangle$  measured in a stirred-grid experiment by Hannoun *et al.* (1988): ◆, close to a sharp density interface (figure 10 of the original paper); ●, close to a solid plate (figure 14 of the original paper). The flux is normalized by its value  $-\langle \mathcal{H} v' \rangle_\infty$  at the same location in the non-stratified situation; the dashed lines represent the two asymptotic regimes  $\langle \mathcal{H} v' \rangle / \langle \mathcal{H} v' \rangle_\infty \propto \mathcal{Y}$  and  $\langle \mathcal{H} v' \rangle / \langle \mathcal{H} v' \rangle_\infty = 1$ , respectively.

$\langle v_s \rangle(\mathcal{Y}) = \langle \mathcal{H} v' \rangle / \langle \mathcal{H} \rangle$ ) can then be performed near  $\mathcal{Y} = 0$ , indicating that at leading order  $v_s(\mathcal{Y})$  varies linearly with the distance to the surface. Consequently, for  $\mathcal{Y} / L_\infty \ll 1$ ,  $v_s(\mathcal{Y})$  evolves as  $v_s(\mathcal{Y}) \sim S(v_\infty) u_\infty \mathcal{Y} / L_\infty$ . Furthermore, assuming that the scaling laws derived in the case of homogeneous undisturbed turbulence remain locally applicable, we know from (A 9) and (A 13) that close to the surface  $v^2 \sim \epsilon_\infty^{2/3} \mathcal{Y}^{2/3}$ , whereas for  $i \neq 2$   $v_i^2 \sim u_\infty^2 - \mu \epsilon_\infty^{2/3} \mathcal{Y}^{2/3} + \eta \epsilon_\infty^{2/3} L_\infty^{-1/3} \mathcal{Y}$ ,  $\mu$  and  $\eta$  being positive numerical constants. Combining these estimates yields

$$\langle v_i^2 v' \rangle \sim S(v_\infty) u_\infty^3 \frac{\mathcal{Y}}{L_\infty} \left[ 1 - \mu' \left( \frac{\mathcal{Y}}{L_\infty} \right)^{2/3} + \eta' \left( \frac{\mathcal{Y}}{L_\infty} \right) \right] \quad \text{for } i \neq 2, \quad (28a)$$

$$\langle v_i^2 v' \rangle \sim S(v_\infty) u_\infty^3 \left( \frac{\mathcal{Y}}{L_\infty} \right)^{5/3} \quad \text{for } i = 2, \quad (28b)$$

where  $\mu'$  and  $\eta'$  are numerical constants proportional to  $\mu$  and  $\eta$ , respectively. Note that if we apply the above reasoning outside the surface-influenced layer, we obtain  $v_s(\mathcal{Y}) \sim S(v_\infty) u_\infty$  and  $v_i^2 \sim u_\infty^2$ , which yields the correct prediction  $\langle v_i^2 v' \rangle \sim S(v_\infty) u_\infty^3$  ( $i = 1, 2, 3$ ). Equation (28b) suggests that the vertical component of the flux is small near the surface since  $-\mathrm{d}\langle v^3 \rangle / \mathrm{d}\mathcal{Y} = O(\epsilon_\infty Re_\infty^{-1/3})$  for  $\mathcal{Y} / L_\infty = O(Re_\infty^{-1/2})$ . In contrast, the leading-order term of (28a) yields a constant flux  $-\mathrm{d}\langle v_i^2 v' \rangle / \mathrm{d}\mathcal{Y} = O(\epsilon_\infty)$  for  $i \neq 2$ . The existence of a constant turbulent flux in the region  $\mathcal{Y} / L_\infty \rightarrow 0$  is strongly supported by the measurements of Hannoun *et al.* (1988), either in the presence of a density interface or near a rigid plate (figure 4). The above predictions can also be compared in more detail with the profiles of the turbulent transport terms found in the LES of CM. These profiles are plotted in figure 5. They confirm that the vertical flux decreases sharply compared to the horizontal flux near the top of the source layer; the  $\mathcal{Y}^{2/3}$  dependence obtained by differentiating (28b) is approximately

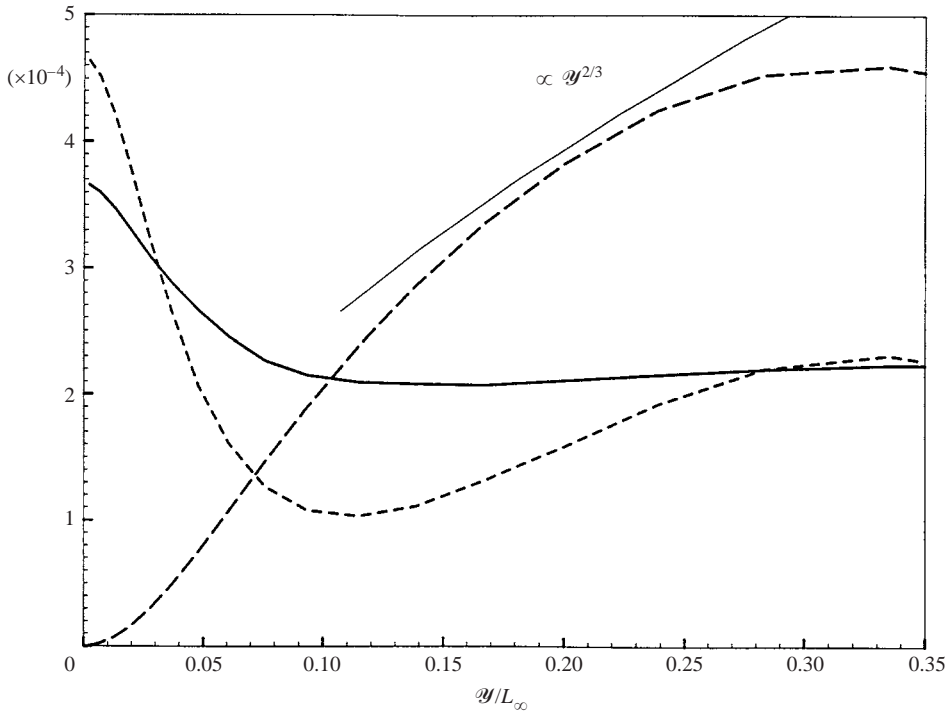


FIGURE 5. The turbulent fluxes near the surface of a high-Reynolds-number steady open-channel flow ( $Re_\infty \approx 360$ ) as found in a LES by Calmet & Magnaudet (2003). The fluxes are normalized by  $\nu/u_*^4$ , where  $u_*$  is the friction velocity at the bottom wall. —, Streamwise component; ---, spanwise component; — · —, vertical component.

observed for  $0.15 \leq y/L_\infty \leq 0.25$  (in this LES,  $Re_\infty \approx 360$  and the viscous sublayer corresponds to  $y/L_\infty \leq 0.1$ , implying a sharper decay of the vertical flux for small values of  $y/L_\infty$ ). The streamwise flux is also found to remain almost constant in accordance with the leading-order term of (28a). The spanwise component is nearly equal to the streamwise one for  $y/L_\infty \approx 0.08$  and  $y/L_\infty > 0.27$  but evolves somewhat differently in between, where a significant reduction is observed. The last two terms on the right-hand side of (28a) are certainly responsible for this behaviour and we believe that the difference between the streamwise and spanwise fluxes has the same origin as the difference observed between the two horizontal r.m.s. velocities in figure 12 of CM.†

To close the above model, we use the LES results reported by CM. More precisely, we consider the ‘free-stream’ values  $u_\infty = u$ , with the value of  $u$  determined in § 5.1 of CM, and  $S(v_\infty) = -0.3$  which corresponds to the value of the skewness factor of the normal velocity measured at  $y/L_\infty = O(1)$ . With these values, the best fit between the model and the LES results is obtained by introducing a numerical constant close to 0.5 (resp. 1.5) in front of the right-hand side of (28a) (resp. (28b)). If these constants are regarded as universal, predictions for the pressure–strain correlations in the limit

† In CM the discussion of § 5.2 suggests that in open-channel flows, the effects of the mean shear result in a larger value of  $\eta'$  in the streamwise component. To account properly for this anisotropy in (28a), it would be necessary to modify the value of  $\eta'$  corresponding to turbulence axisymmetric about the  $y$ -axis by a correction involving the non-zero value of the skewness factor  $S(u_\infty)$  associated with the streamwise velocity fluctuation.

$\mathcal{Y}/L_\infty \rightarrow 0$  can be obtained for purely diffusive turbulence. Assuming that the results of Appendix A remain approximately applicable, we may write at leading order  $\epsilon_{ii}(\mathcal{Y}) \approx (2/3)\epsilon_\infty(\mathcal{Y})$  (no summation on  $i$ ). Then, applying the approximate relation  $\epsilon_\infty = u_\infty^3/(2L_\infty)$  valid for isotropic turbulence (Tennekes & Lumley 1972, p. 273), we obtain  $\epsilon_{ii}(\mathcal{Y}) \approx u_\infty^3(\mathcal{Y})/(3L_\infty(\mathcal{Y}))$ . Incorporating the above features of the model in (27), we find at leading order

$$\phi_{ii}(\mathcal{Y}/L_\infty \rightarrow 0) \approx \epsilon_\infty(0) \left[ \frac{2}{3} + S(v_\infty) \right] \quad \text{for } i \neq 2. \quad (29)$$

Using (28*a, b*) in the turbulent kinetic energy balance, we also obtain an estimate of the surface value of the pressure–diffusion flux, namely

$$-\left( \frac{\partial}{\partial \mathcal{Y}} \left\langle \frac{p'}{\rho} v' \right\rangle \right) (\mathcal{Y}/L_\infty \rightarrow 0) \approx \epsilon_\infty(0) [1 + S(v_\infty)]. \quad (30)$$

Equations (29) and (30) show that the sign of the surface values of the pressure–strain correlations and of the pressure–diffusion flux depends directly on the value of the skewness factor  $S(v_\infty)$  assumed to govern the leading-order contribution to the turbulent transport; nevertheless the critical value  $S(v_\infty) = -2/3$  for which the right-hand side of (29) changes sign must be regarded as indicative at this stage. Owing to the moderate values ( $-0.3$  to  $-0.4$ ) of  $S(v_\infty)$  found in high-Reynolds-number open-channel flows (Nakagawa & Nezu 1977), (29) and (30) predict that the pressure–diffusion flux and the tangential components of  $\phi_{ii}$  are both positive in this type of flow. This prediction agrees with the numerical results displayed in figures 5(*b*) and 6 of CM. According to the literature, skewness factors have not been determined in stirred-grid tank experiments. Nevertheless Hannoun *et al.* (1988) reported the turbulent flux  $-\langle \mathcal{K} v' \rangle$  replotted in figure 4, from which  $S(v_\infty)$  can be estimated provided the cross-correlation coefficient  $\langle v_i'^2 v' \rangle / (\langle v_i'^2 \rangle \langle v'^2 \rangle^{1/2})$  ( $i \neq 2$ ) is known. Assuming that this coefficient lies between  $S(v_\infty)/3$ , as found in shearless mixing layers (Veeravalli & Warhaft 1989), and  $S(v_\infty)/2$ , as observed in diffusive turbulence produced by a confined jet (Risso & Fabre 1997), these data indicate averaged values of  $|S(v_\infty)|$  in the range  $0.62 \pm 0.04$ .<sup>†</sup> According to (29),  $\phi_{ii}(\mathcal{Y}/L_\infty \rightarrow 0)$  ( $i \neq 2$ ) is then close to zero; hence we guess that the surface-induced intercomponent energy transfer is small in high-Reynolds-number stirred-grid turbulence.

According to our model, intercomponent energy transfer within the surface-influenced layer of flows in which  $|S(v_\infty)| > 2/3$  should be dominated by the isotropization mechanism described in §4.2. However, we are not aware of situations of diffusive turbulence in which  $|S(v_\infty)|$  reaches such high values, so that we cannot check this prediction. Nevertheless, the most important point in the present context is that combining a crude model of the asymmetry of the large-scale normal motions with the HG predictions for the velocity variances results in a model of third-order moments from which negative values of  $\phi_{22}$  are predicted for moderate values of  $S(v_\infty)$ . Considering this conclusion together with the results previously obtained in the case of freely evolving turbulence shows that the HG theory does not conflict with any of the physical mechanisms of intercomponent energy transfer near a flat surface reported to date.

<sup>†</sup> Interestingly, combining this estimate with the slope of figure 4 and the experimental profile of the undisturbed turbulent flux  $-\langle \mathcal{K} v' \rangle_\infty(\mathcal{Y})$  confirms the value of approximately 0.5 for the empirical constant in front of the right hand-side of (28*a*).

## 5. Summary and concluding remarks

As the capability of the HG theory to predict turbulent statistics at large time following the sudden insertion of a flat surface has been seriously questioned in recent years, we have re-examined this question in detail. Our plan was to determine the order of magnitude of the vortical corrections produced by the strain associated with the large-scale eddies impinging on the surface. An estimate of these corrections was obtained by considering the enstrophy budget and balancing the stretching term by nonlinear contributions and dissipation. The resulting estimate indicates that the relative magnitude of the vortical corrections is proportional to  $Re_\infty^{-1}$  and has a maximum value of order  $Re_\infty^{-1/3}$  in the part of the source layer closest to the surface. This argument supports the validity of the HG theory at large time in the high-Reynolds-number limit and predicts a nonlinear amplification of tangential r.m.s. velocities smaller than Hunt's (1984) correction. It explains why experiments performed in stirred-grid tanks or LES results reported in CM agree quantitatively well with the HG predictions and why significant discrepancies can be observed when the turbulent Reynolds number is low, as is usually the case in DNS studies.

Based on this result, we showed that a leading-order expression for the pressure disturbance induced by the surface can be derived from the full Navier–Stokes equations without neglecting the main nonlinearities or the viscous term. Therefrom, transport equations for the Reynolds stresses were formed and their implications were studied within the framework of the HG approximation. Analytical results show that at the time when the surface is inserted,  $\phi_{22}$  is negative and the pressure–diffusion flux lowers the turbulent kinetic energy within the surface-influenced layer. In the case of freely decaying turbulence, further evolution is dominated by the imbalance between dissipation (which is essentially left unaltered by the surface) and time-rate-of-change of the energy components, resulting in a positive value of  $\phi_{22}$  ranging from zero at the outer limit of the source layer to  $\frac{2}{3}\epsilon_\infty$  at the edge of the viscous sublayer. The positive sign of  $\phi_{22}$  corresponds to an isotropization process and agrees with available DNS results; moreover it does not contradict the fact that the tangential velocity variances near the surface exceed their free-stream value at any time.

We finally considered the more complex case of steady spatially decaying turbulence in which intercomponent energy transfer is governed by turbulent fluxes associated with third-order moments. We derived a physically based model of the vertical turbulent fluxes incorporating some basic features resulting from the HG theory and we fitted this model using LES data. For moderate levels of inhomogeneity, the model predicts a negative surface value of  $\phi_{22}$ , indicating that energy is transferred from the normal velocity component towards the tangential components, in agreement with numerical results available for open-channel flow.

Combining numerical results available for time decaying and spatially decaying turbulence, it turns out that the intercomponent energy transfer near a flat surface depends crucially on the nature (steady vs. decaying, homogeneous vs. inhomogeneous) of the outer turbulence. In the present investigation we only considered the case where this turbulence is (at least locally) isotropic. There is no doubt that if some anisotropy is present in the free stream, it may also affect crucially the intercomponent energy transfer (e.g. Wong 1985). The present analytical conclusions suggest that the HG theory, combined with suitable closures of third-order moments in the case where the outer turbulence is inhomogeneous in the  $\mathcal{Y}$ -direction, is able to encompass this variety of situations. Another implication of our analysis concerns one-point turbulence models. It has been proposed in the past that intercomponent energy transfer due to an impermeable surface can be modelled within the framework of second-order

closures by adding an ‘echo’ term to the closure of the pressure–strain tensor (Launder, Reece & Rodi 1975; Hanjalic & Launder 1976; Gibson & Launder 1978; Shih & Lumley 1986). In most attempts this echo term was assumed to depend only on the local anisotropy of the Reynolds stress tensor and on the distance to the surface. Given the HG distribution of the velocity variances, such models predict negative surface-induced values of  $\phi_{22}$  in the situation considered in §4.2 as well as in that of §4.3, and these values are identical in both cases. The present analytical predictions and DNS/LES results indicate that in general such predictions are incorrect. Consequently it appears that properties of the incoming turbulence have to be taken into account in the modelling of the surface-induced contributions to the pressure–strain tensor. An interesting attempt in this direction was proposed by Durbin (1993) whose elliptic model is able to capture non-local effects.

This work was made possible by the inspiring source provided by the PhD work of I. Calmet. I am greatly indebted to her for her continuous collaboration and welcome suggestions. I am also very grateful to J. P. Bertoglio, P. Carlotti, J. C. R. Hunt and F. Risso for stimulating and enlightening discussions on different parts of this work, and to Victor<sup>©</sup> for providing me with fine daily examples of high-Reynolds-number free-surface turbulence.

### Appendix A. Velocity gradients within the source layer

The rapid distortion theory was extended to turbulence distorted by a two-dimensional bluff body by Hunt (1973), and subsequently to turbulence distorted by a flat surface by HG. In the latter case, short-time RDT assumptions imply that the velocity fluctuation  $\mathbf{v}'(x, \mathcal{Y}, z, t)$  at a distance  $\mathcal{Y}$  from the surface simply differs from the free-stream fluctuation  $\mathbf{v}_\infty(x, \mathcal{Y}, z, t)$  by an irrotational fluctuation  $\nabla\Phi(x, \mathcal{Y}, z, t)$ . Hunt (1973) showed that the two-dimensional Fourier transforms  $\hat{\Phi}(k_1, k_3, \mathcal{Y}, t)$  and  $\hat{v}'_i(k_1, k_3, \mathcal{Y}, t)$  of the velocity potential  $\Phi$  and velocity fluctuation  $\mathbf{v}'$  are related to the three-dimensional Fourier transform  $\hat{v}_\infty(\mathbf{k}, t)$  of the free-stream velocity fluctuation through

$$\hat{\Phi}(k_1, k_3, \mathcal{Y}, t) = \int_{-\infty}^{+\infty} \beta_m(\mathbf{k}, \mathcal{Y}) \hat{v}_{m\infty}(\mathbf{k}, t) dk_2, \tag{A 1a}$$

$$\hat{v}'_i(k_1, k_3, \mathcal{Y}, t) = \int_{-\infty}^{+\infty} M_{im}(\mathbf{k}, \mathcal{Y}) \hat{v}_{m\infty}(\mathbf{k}, t) dk_2, \tag{A 1b}$$

where  $k_1, k_2$  and  $k_3$  are the components of the wavenumber  $\mathbf{k}$  along directions  $x, \mathcal{Y}$  and  $z$  respectively. From the relation  $\mathbf{v}' = \mathbf{v}_\infty + \nabla\Phi$  it is immediately apparent that the ‘distortion’ tensor  $M_{im}$  is given by

$$M_{im}(\mathbf{k}, \mathcal{Y}) = \delta_{im} e^{ik_2\mathcal{Y}} + \begin{bmatrix} ik_1\beta_m(\mathbf{k}, \mathcal{Y}) \\ \partial\beta_m(\mathbf{k}, \mathcal{Y})/\partial\mathcal{Y} \\ ik_3\beta_m(\mathbf{k}, \mathcal{Y}) \end{bmatrix}, \tag{A 1c}$$

with  $i^2 = -1$ . If turbulence is homogeneous in planes  $(x, z)$  parallel to the surface, the Laplace equation (5) becomes in Fourier space

$$\left[ \frac{\partial^2}{\partial\mathcal{Y}^2} - k_H^2 \right] \hat{\Phi}(k_1, k_3, \mathcal{Y}, t) = 0,$$

$k_H = (k_1^2 + k_3^2)^{1/2}$  being the tangential wavenumber. The solution of this equation satisfying boundary conditions (7b) and (11) is  $(e^{-k_H \mathcal{Y}}/k_H) \int_{-\infty}^{+\infty} \hat{v}_\infty(\mathbf{k}, t) dk_2$ ,  $\hat{v}_\infty$  being the normal component of  $\hat{\mathbf{v}}_\infty(\mathbf{k}, t)$ . Comparing with (A1a) yields, after HG,

$$\beta_m(\mathbf{k}, \mathcal{Y}) = \frac{1}{k_H} e^{-k_H \mathcal{Y}} \delta_{m2}. \quad (\text{A } 2)$$

From (A1)–(A2) one deduces that the variance of the components of the velocity gradient tensor  $\langle\langle (\partial v'_i / \partial x_j)^2 \rangle\rangle$  (no summation on  $i$  or  $j$ ) is related to the three-dimensional velocity spectrum  $\Phi_{ij}(\mathbf{k})$  of the free-stream turbulence through

$$\langle\langle (\partial v'_i / \partial x_j)^2 \rangle\rangle = \begin{cases} \int_{-\infty}^{+\infty} k_j^2 M_{im}^*(\mathbf{k}, \mathcal{Y}) M_{in}(\mathbf{k}, \mathcal{Y}) \Phi_{mn}(\mathbf{k}) d^3 \mathbf{k} & \text{for } j \neq 2, \\ \int_{-\infty}^{+\infty} \frac{\partial M_{im}^*(\mathbf{k}, \mathcal{Y})}{\partial \mathcal{Y}} \frac{\partial M_{in}(\mathbf{k}, \mathcal{Y})}{\partial \mathcal{Y}} \Phi_{mn}(\mathbf{k}) d^3 \mathbf{k} & \text{for } j = 2, \end{cases} \quad (\text{A } 3)$$

where  $d^3 \mathbf{k} = dk_1 dk_2 dk_3$  and the star denotes the complex conjugate. Inserting (A1 a–c) into (A3) yields

$$\begin{aligned} & \langle\langle (\partial v'_i / \partial x_j)^2 \rangle\rangle \\ = & \begin{cases} \int_{-\infty}^{+\infty} k_j^2 \left\{ \Phi_{ii}(\mathbf{k}) + 2 \frac{k_i}{k_H} \sin(k_2 \mathcal{Y}) e^{-k_H \mathcal{Y}} \Phi_{i2}(\mathbf{k}) + \frac{k_i^2}{k_H^2} e^{-2k_H \mathcal{Y}} \Phi_{22}(\mathbf{k}) \right\} d^3 \mathbf{k}, & i \neq 2, j \neq 2, \\ \int_{-\infty}^{+\infty} k_j^2 \{ 1 - 2 \cos(k_2 \mathcal{Y}) e^{-k_H \mathcal{Y}} + e^{-2k_H \mathcal{Y}} \} \Phi_{22}(\mathbf{k}) d^3 \mathbf{k}, & i = 2, j \neq 2, \\ \int_{-\infty}^{+\infty} \{ k_2^2 \Phi_{ii}(\mathbf{k}) - 2k_i k_2 \cos(k_2 \mathcal{Y}) e^{-k_H \mathcal{Y}} \Phi_{i2}(\mathbf{k}) + k_i^2 e^{-2k_H \mathcal{Y}} \Phi_{22}(\mathbf{k}) \} d^3 \mathbf{k}, & i \neq 2, j = 2, \\ \int_{-\infty}^{+\infty} \{ k_2^2 - 2k_2 k_H \sin(k_2 \mathcal{Y}) e^{-k_H \mathcal{Y}} + k_H^2 e^{-2k_H \mathcal{Y}} \} \Phi_{22}(\mathbf{k}) d^3 \mathbf{k}, & i = 2, j = 2. \end{cases} \end{aligned} \quad (\text{A } 4)$$

Equations (A1)–(A3) reveal that terms involving  $e^{-2k_H \mathcal{Y}}$  in (A4) correspond to the contribution  $\langle\langle (\partial^2 \Phi / \partial x_i \partial x_j)^2 \rangle\rangle$  whereas terms involving  $e^{-k_H \mathcal{Y}}$  correspond to velocity gradients produced by the interaction between the free-stream fluctuation and the perturbation  $\nabla \Phi$ .

In what follows we consider that the free-stream turbulence is homogeneous and isotropic. Since the essential contribution to the velocity gradients comes from the high-wavenumber part of the spectrum, we approximate  $\Phi_{mn}(\mathbf{k})$  by a Kolmogorov spectrum with a sharp cut-off at the Kolmogorov wavenumber  $k_K = ((2/3)C_K(\epsilon_\infty^{1/3}/\nu))^{3/4}$ , so that

$$\Phi_{mn}(\mathbf{k}) = C_K \epsilon_\infty^{2/3} (k^2 \delta_{mn} - k_m k_n) k^{-17/3} \quad \text{for } k \leq k_K, \quad (\text{A } 5)$$

where  $C_K$  is the Kolmogorov constant,  $k = \|\mathbf{k}\|$ , and  $\epsilon_\infty$  is the dissipation rate in the free stream. Note that, since (A5) does not describe correctly the energy distribution at low wavenumber, it cannot be used to predict the distortion produced by the surface at distances such that  $\mathcal{Y}/L_\infty = O(1)$ . Consequently, the results derived in this Appendix are essentially valid in the limit  $\mathcal{Y}/L_\infty \rightarrow 0$ .

For  $\mathcal{Y}/L_\infty$  large compared to unity, terms involving  $e^{-k_H \mathcal{Y}}$  and  $e^{-2k_H \mathcal{Y}}$  are negligible in (A 4). Under such conditions one recovers the well-known result (Monin & Yaglom 1975, p. 56)

$$\langle (\partial v'_i / \partial x_j)^2 \rangle_\infty = \frac{\epsilon_\infty / \nu}{15} \begin{bmatrix} 1 & 2 & 2 \\ 2 & 1 & 2 \\ 2 & 2 & 1 \end{bmatrix}. \quad (\text{A } 6)$$

In the limit  $Re_\infty \rightarrow \infty$ ,  $k_K L_\infty$  is of order  $Re_\infty^{3/4}$  (Monin & Yaglom 1975, p. 349) and  $\mathcal{Y}/L_\infty$  is of order  $Re_\infty^{-1/2}$  for  $\mathcal{Y} = O(\delta_V)$ . Hence the source layer of the HG theory corresponds typically to  $k_K \mathcal{Y}$  ranging from the order  $Re_\infty^{1/4}$  to the order  $Re_\infty^{3/4}$ . To obtain the variance of velocity gradients in the part of this layer closest to the surface, we thus consider the intermediate limit  $k_K \mathcal{Y} \rightarrow \infty$ ,  $\mathcal{Y}/L_\infty \rightarrow 0$ . Under such conditions, (A 1*b,c*) show that eddies with tangential wavenumbers typically smaller than  $1/\mathcal{Y}$  are distorted by the surface whereas eddies with  $1/\mathcal{Y} \leq k_H \leq k_K$  are almost unaltered. Expressions (A 4) may then be evaluated analytically in this intermediate limit by using the properties of the Gamma function (Abramowitz & Stegun 1965, p. 374) and integrating analytically hypergeometric functions (Abramowitz & Stegun 1965, p. 258–260; Gradshteyn & Ryzhik 1980, p. 712). After lengthy algebra we obtain the final result†

$$\langle (\partial v'_i / \partial x_j)^2 \rangle(\mathcal{Y}) \approx \frac{\epsilon_\infty / \nu}{15} \begin{bmatrix} 1 & 2 & 2 \\ 2 & 1 & 2 \\ 2 & 2 & 1 \end{bmatrix} + \frac{\epsilon_\infty / \nu}{(k_K \mathcal{Y})^{4/3}} \begin{bmatrix} \sim 0 & 0.116 & \sim 0 \\ -0.201 & 0 & -0.201 \\ \sim 0 & 0.116 & \sim 0 \end{bmatrix}. \quad (\text{A } 7)$$

Since  $k_K \mathcal{Y}$  is large in the source layer, (A 7) indicates that the presence of the surface has a negligible influence on  $\langle (\partial v'_i / \partial x_j)^2 \rangle$  for  $i \neq 2$  and  $j \neq 2$ , as well as on  $\langle (\partial v' / \partial \mathcal{Y})^2 \rangle$ . In particular it is worth noting that for  $\mathcal{Y} = O(\delta_V)$ ,  $\langle (\partial v' / \partial \mathcal{Y})^2 \rangle$  is almost identical to its free-stream value while, according to the result of HG and to (A 9) below, the value of  $\langle v'^2 \rangle$  is reduced by a factor of order  $(\mathcal{Y}/L_\infty)^{-2/3} = O(Re_\infty^{1/3})$ . From (A 7) we also see that  $\langle (\partial u' / \partial \mathcal{Y})^2 \rangle$  and  $\langle (\partial w' / \partial \mathcal{Y})^2 \rangle$  increase as the surface is approached, while  $\langle (\partial v' / \partial x)^2 \rangle$  and  $\langle (\partial v' / \partial z)^2 \rangle$  are reduced. Summation of results (A 7) over  $i$  and  $j$  shows that the local pseudo-dissipation per unit mass is

$$\epsilon(\mathcal{Y}) = \epsilon_\infty (1 - 0.173(k_K \mathcal{Y})^{-4/3}). \quad (\text{A } 8)$$

Hence RDT predicts that the pseudo-dissipation is slightly reduced in the source layer. In contrast, since in this approach the difference between the local value and the undisturbed value of the velocity fluctuation reduces to an irrotational field, the variance of vorticity fluctuations is not modified by the surface. Interestingly, the kinematic relation  $S^2 = \epsilon(\mathcal{Y})/\nu - \partial^2 \langle v'^2 \rangle / \partial \mathcal{Y}^2$  linking the local value of the pseudo-dissipation  $\epsilon(\mathcal{Y})$  to the enstrophy  $S^2/2$  can be used to recover the near-surface evolution of  $\langle v'^2 \rangle$ . Combining (A 8) with the fact that  $S^2 = \epsilon_\infty / \nu$  everywhere yields, after integrating twice and requiring that  $\langle v'^2 \rangle \rightarrow 0$  for  $\mathcal{Y} \rightarrow 0$ ,

$$\langle v'^2 \rangle(\mathcal{Y}) = 1.784 \epsilon_\infty^{2/3} \mathcal{Y}^{2/3} + O(\epsilon_\infty^{2/3} L_\infty^{-1/3} \mathcal{Y}), \quad (\text{A } 9)$$

where we have set  $C_K = 0.25 \frac{55}{9} \approx 1.528$  (Townsend 1976, p. 98). The leading-order term in (A 9) agrees with the result found by Hunt (1984). Note that this term is independent of the low-wavenumber part of the energy spectrum, since only the

† Detail of calculations may be obtained on request from the author or the Journal of Fluid Mechanics editorial office, Cambridge.

high-wavenumber shape was specified in (A 5). Moreover, expanding the product  $M_{22}(\mathbf{k}, \mathscr{Y})M_{22}^*(\mathbf{k}, \mathscr{Y})$  in the limit  $k\mathscr{Y} \rightarrow 0$  shows that the contribution of low wavenumbers to  $\langle v'^2 \rangle(\mathscr{Y})$  is of order  $\mathscr{Y}^2$ , i.e. the linear term in (A 9) is actually zero.

To determine  $\partial^2 \langle v_i'^2 \rangle / \partial \mathscr{Y}^2$  ( $i \neq 2$ ) in the limit  $\mathscr{Y}/L_\infty \rightarrow 0$ , let us begin by evaluating

$$\left\langle v_i' \frac{\partial^2 v_i'}{\partial \mathscr{Y}^2} \right\rangle = \int_{-\infty}^{+\infty} M_{im}^*(\mathbf{k}, \mathscr{Y}) \frac{\partial^2 M_{in}(\mathbf{k}, \mathscr{Y})}{\partial \mathscr{Y}^2} \Phi_{mn}(\mathbf{k}) d^3 \mathbf{k}. \quad (\text{A } 10)$$

Using (A 1c), (A 2) and intermediate results obtained during the evaluation of (A 7), we find

$$\left\langle v_i' \frac{\partial^2 v_i'}{\partial \mathscr{Y}^2} \right\rangle \approx -\frac{2}{15} \epsilon_\infty / \nu + \frac{18}{455} \Gamma(1/3) \frac{\epsilon_\infty / \nu}{(k_K \mathscr{Y})^{4/3}}, \quad (\text{A } 11)$$

where  $\Gamma$  denotes the Gamma function. Now, adding results (A 7) (for  $i \neq 2$  and  $j = 2$ ) and (A 11), we find

$$\frac{\partial^2 \langle v_i'^2 \rangle}{\partial \mathscr{Y}^2} = 2 \left( \left\langle v_i' \frac{\partial^2 v_i'}{\partial \mathscr{Y}^2} \right\rangle + \left\langle \left( \frac{\partial v_i'}{\partial \mathscr{Y}} \right)^2 \right\rangle \right) \approx 0.372 \frac{\epsilon_\infty / \nu}{(k_K \mathscr{Y})^{4/3}} \quad \text{for } i \neq 2. \quad (\text{A } 12)$$

This result can also be used to obtain the leading-order terms governing the variations of  $\langle v_i'^2 \rangle$  ( $i \neq 2$ ) in the limit  $\mathscr{Y}/L_\infty \rightarrow 0$ . Integrating twice and requiring that the surface value of  $\langle v_i'^2 \rangle$  matches the kinetic energy found at  $\mathscr{Y} = 0$  in (22) implies

$$\langle u'^2 \rangle = \langle w'^2 \rangle = \frac{3}{2} u^2 - 3.838 \epsilon_\infty^{2/3} \mathscr{Y}^{2/3} + O(\epsilon_\infty^{2/3} L_\infty^{-1/3} \mathscr{Y}). \quad (\text{A } 13)$$

Expanding the products  $M_{ip}(\mathbf{k}, \mathscr{Y})M_{iq}^*(\mathbf{k}, \mathscr{Y})$  involved in the expression for  $\langle v_i'^2 \rangle(\mathscr{Y})$  in the limit  $k\mathscr{Y} \rightarrow 0$  reveals that low wavenumbers provide a non-zero linear contribution to the variance of the tangential fluctuations. The exact magnitude of this contribution depends of the shape of the energy spectrum in the low-wavenumber range; its sign is always positive, implying the existence of a minimum of the tangential r.m.s. velocities within the source layer.

Equations (A 7), (A 9) and (A 13) can be used to deduce the evolution of the Taylor microscales within the source layer. Since  $\langle u'^2 \rangle$  and  $\langle w'^2 \rangle$  increase by a factor of 3/2 when  $\mathscr{Y}$  ranges from a value of order  $L_\infty$  to a value of order  $Re_\infty^{-1/2} L_\infty$ , the longitudinal and transverse microscales of the tangential fluctuations increase by a factor  $(3/2)^{1/2} \approx 1.22$ . In contrast, since  $\langle v'^2 \rangle$  decreases by a factor  $Re_\infty^{1/3}$  between  $\mathscr{Y} = O(L_\infty)$  and  $\mathscr{Y} = O(L_\infty Re_\infty^{-1/2})$ , the transverse microscale associated with the normal velocity,  $\lambda_{2T}$ , decreases by a factor of order  $Re_\infty^{1/6}$ . More precisely, using (A 9) we find that for  $\mathscr{Y}/L_\infty = 2Re_\infty^{-1/2}$ ,  $\lambda_{2T}$  decreases by  $(1.78)^{-1/2} Re_\infty^{1/6}$  compared to its free-stream value. These results compare well with the numerical evolutions of the Taylor microscales obtained by WLGR.

## Appendix B. Pressure–velocity and pressure–strain correlations at $t = 0$

Since the surface is suddenly inserted in the flow at  $t = 0$ , the irrotational correction  $\nabla \Phi$  is zero for  $t < 0$ . For  $t > 0$ , the two-dimensional Fourier transform of  $\Phi$  is given by (A 1a) and (A 2). Consequently the velocity potential may be written at any time in the form

$$\hat{\Phi}(k_1, k_3, \mathscr{Y}, t) = H(t) \frac{e^{-k_H \mathscr{Y}}}{k_H} \int_{-\infty}^{+\infty} \hat{v}_\infty(\mathbf{k}, t) dk_2, \quad (\text{B } 1)$$

where  $H(t)$  is the Heaviside distribution. Equations (B 1) and (A 1a) give the normal velocity fluctuation as

$$\hat{v}'(k_1, k_3, \mathscr{Y}, t) = \int_{-\infty}^{+\infty} [e^{ik_2\mathscr{Y}} - H(t)e^{-k_H\mathscr{Y}}] \hat{v}_\infty(\mathbf{k}, t) dk_2. \quad (\text{B } 2)$$

From (19) it is clear that the pressure fluctuation at  $t = 0$  is dominated by the singular term  $-\rho\partial\Phi/\partial t$ . Thus the leading-order contribution to the Fourier transform of the initial pressure fluctuation  $p'(X, t \rightarrow 0)$  is, according to (B 1),

$$\hat{p}'(k_1, k_3, \mathscr{Y}, t \rightarrow 0) \approx -\rho\delta(t) \frac{e^{-k_H\mathscr{Y}}}{k_H} \int_{-\infty}^{+\infty} \hat{v}_\infty(\mathbf{k}, t) dk_2, \quad (\text{B } 3)$$

where  $\delta(t)$  is the Dirac distribution. Using (B 2) and (B 3), the initial value of the pressure–diffusion flux is found to be

$$\begin{aligned} -\frac{1}{\rho} \frac{\partial \langle p'v' \rangle}{\partial \mathscr{Y}}(\mathscr{Y}, t \rightarrow 0) &\approx \delta(t) \int_{-\infty}^{+\infty} \Phi_{22}(\mathbf{k}) \\ &\times \left[ 2H(t)e^{-2k_H\mathscr{Y}} - \left( \cos(k_2\mathscr{Y}) + \frac{k_2}{k_H} \sin(k_2\mathscr{Y}) \right) e^{-k_H\mathscr{Y}} \right] d^3\mathbf{k}. \end{aligned} \quad (\text{B } 4)$$

From (B 4) the integral of the pressure–diffusion term from  $t = 0^-$  to  $t = 0^+$  can be evaluated by noting that

$$\int_{t=0^-}^{t=0^+} \delta(t)H(t) dt = \int_{t=0^-}^{t=0^+} H'(t)H(t) dt = 1/2.$$

It is immediately apparent that the resulting quantity is zero at the surface and a Taylor expansion shows that it is negative for all  $\mathscr{Y}$  for wavenumbers such that  $k\mathscr{Y} \ll 1$ . Since low wavenumbers dominate the integral in (B 4), one can infer that the time integral of the pressure–diffusion flux is negative throughout the surface-influenced layer. Using (B 2)–(B 3), the pressure–strain correlation in the vertical direction is also found to be

$$\left\langle \frac{p'}{\rho} \frac{\partial v'}{\partial \mathscr{Y}} \right\rangle(\mathscr{Y}, t \rightarrow 0) \approx \delta(t) \int_{-\infty}^{+\infty} \Phi_{22}(\mathbf{k}) \left[ \frac{k_2}{k_H} e^{-k_H\mathscr{Y}} \sin(k_2\mathscr{Y}) - H(t)e^{-2k_H\mathscr{Y}} \right] d^3\mathbf{k}. \quad (\text{B } 5)$$

By a similar argument it is straightforward to show that the integral of this term from  $t = 0^-$  to  $t = 0^+$  is also negative everywhere.

### Appendix C. Revisiting Hunt’s (1984) nonlinear correction

Hunt (1984) derived a nonlinear correction to the original HG theory from a formal analogy with results obtained by Durbin (1981) in the analysis of the rapid distortion of turbulence near the front stagnation point of a sphere. In the situation considered by Durbin, a turbulent field with characteristic intensity  $\mathscr{V}_\infty$  and integral length scale  $l_\infty$  is convected towards a sphere of radius  $R$  by a mean flow of speed  $U_\infty$  far upstream. The changes in the mean flow due to the presence of the sphere produce strains of order  $U_\infty/R$  close to the sphere surface; these strains distort the turbulent vorticity field, resulting in a change  $(\Delta\mathscr{V})^2$  of velocity variances. Durbin evaluated analytically  $(\Delta\mathscr{V}^2)$  in the limit case of ‘small-scale turbulence’ (Hunt 1973) for which the mean flow variations are negligibly small over one integral length scale, i.e.  $l_\infty/R \ll 1$ . He found that at a distance  $d$  from the front stagnation point such that  $d/R \ll 1$ , all three velocity variances are amplified by an order  $\mathscr{V}_\infty^2(d/R)^{-1/2}$ , the

amplification of the normal (streamwise) component being twice that of the tangential ones. His analysis excludes the source layer corresponding typically to  $d < l_\infty$ , where the normal velocity falls to zero at the sphere surface. As usual in RDT approaches, Durbin's conclusions are valid under conditions ensuring that nonlinear contributions of large eddies to advection and stretching can be neglected in the vorticity equation, implying  $\mathcal{V}_\infty/U_\infty \ll 1$  and  $\mathcal{V}_\infty/l_\infty \ll U_\infty/R$  (Hunt 1973; Goldstein & Durbin 1980). Summarizing, Durbin's conclusions can be collected in the form

$$(\Delta \mathcal{V})^2 = O \left( \mathcal{V}_\infty^2 \left( \frac{d}{R} \right)^{-1/2} \right) \quad \text{for} \quad \frac{l_\infty}{R} < \frac{d}{R} \ll 1 \quad (\text{C1})$$

provided

$$\frac{\mathcal{V}_\infty}{U_\infty} \ll \frac{l_\infty}{R} \ll 1. \quad (\text{C2})$$

The nonlinear correction derived by Hunt (1984) is based on the idea that Durbin's results are applicable to the source layer near a flat surface, because small-scale eddies of size  $l$  and velocity  $u(l)$  entrained by large eddies impinging on the surface 'feel' the flow due to these eddies as an axisymmetric slowly evolving flow. To check this idea, we may rewrite (C1)–(C2) for the present problem by replacing all quantities by their counterparts. Scales  $\mathcal{V}_\infty$ ,  $l_\infty$  and  $d$  must obviously be replaced by  $u(l)$ ,  $l$  and  $\mathcal{Y}$ , respectively, and the 'mean' flow is now characterized by the r.m.s. velocity far from the surface,  $u_\infty$ . Replacing  $R$  requires a little more physical reasoning. In (C1)  $R$  characterizes the thickness of the region surrounding the sphere where mean velocity gradients are significant. In our problem, the counterpart of this region is the surface-influenced layer whose typical thickness is  $L_\infty$ . In contrast, in (C2)  $R$  appears because mean velocity gradients are of order  $U_\infty/R$  close to the sphere. In Appendix A we showed that the r.m.s. velocity gradients are of order  $u_\infty/(L_\infty^{1/3}\mathcal{Y}^{2/3})$  in the source layer, from which we deduce that  $R$  must be replaced by  $L_\infty^{1/3}\mathcal{Y}^{2/3}$  in (C2). Furthermore we note that small-scale eddies of size  $l$  certainly belong to the inertial subrange, in which case the inertial scaling implies  $u(l) = u_\infty(l/L_\infty)^{1/3}$  (Hunt & Carruthers 1990). Introducing all these scales in (C1)–(C2) gives the change  $(\Delta u)^2$  experienced by the velocity variances near the surface as

$$(\Delta u)^2 = O \left( u_\infty^2 \left( \frac{\mathcal{Y}}{L_\infty} \right)^{-1/2} \right) \quad \text{for} \quad \frac{l}{L_\infty} < \frac{\mathcal{Y}}{L_\infty} \ll 1 \quad (\text{C3})$$

provided

$$\left( \frac{l}{L_\infty} \right)^{1/3} \ll \frac{l}{L_\infty} \left( \frac{L_\infty}{\mathcal{Y}} \right)^{2/3} \ll 1. \quad (\text{C4})$$

We see that the first inequality in (C3) requires  $l/\mathcal{Y} < 1$ , whereas the first inequality in (C4) is equivalent to  $(l/\mathcal{Y})^{2/3} \gg 1$ . Consequently there is no subrange of eddies of size  $l$  where nonlinear stretching and direct influence of the surface can both be neglected. This makes Hunt's (1984) estimate of the amplification of small-scale vorticity in the surface-influenced layer questionable. On the other hand, we note that Hunt (1973) solved the case of small-scale turbulence approaching the front stagnation point of a circular cylinder. His calculation, where both stretching by the mean flow field and blocking by the surface are taken into account, shows that the zero-wavenumber value of the one-dimensional spectrum of the normal velocity is indeed increased by the mean strain rate and behaves as  $(\mathcal{Y}/L_\infty)^{-1/3}$  near the surface (equation (6.36b))

and figure 13 of the original paper). Hence, even though we believe that the direct analogy between Durbin's (1979) results near a sphere and the source layer near a flat surface is questionable, there is no doubt that, if viscous mechanisms are disregarded, nonlinear vortex stretching by large-scale motions leads to an amplification of the velocity variances near the surface.

#### REFERENCES

- ABRAMOWITZ, M. & STEGUN, I. A. 1965 *Handbook of Mathematical Functions*. Dover.
- ARONSON, D., JOHANSSON, A. V. & LÖFDAHL, L. 1997 Shear-free turbulence near a wall. *J. Fluid Mech.* **338**, 363–385.
- BATCHELOR, G. K. 1953 *The Theory of Homogeneous Turbulence*. Cambridge University Press.
- BATCHELOR, G. K. 1967 *An Introduction to Fluid Dynamics*. Cambridge University Press.
- BIRINGEN, S. & REYNOLDS, W. C. 1981 Large-eddy simulation of the shear-free turbulent boundary layer. *J. Fluid Mech.* **103**, 53–63.
- BRUMLEY, B. H. & JIRKA, G. H. 1987 Near surface turbulence in grid-stirred tank. *J. Fluid Mech.* **183**, 235–263.
- CALMET, I. & MAGNAUDET, J. 2003 Statistical structure of high-Reynolds-number turbulence close to the flat free surface of an open-channel flow. *J. Fluid Mech.* **474**, 355–378 (referred to herein as CM).
- CARLOTTI, P. 2001 Distorted turbulence near rigid boundaries. PhD Dissertation, Cambridge University.
- CARLOTTI, P. 2002 Two-point properties of atmospheric turbulence very close to the ground: Comparison of a high resolution LES with theoretical models. *Boundary-Layer Met.* **104**, 381–410.
- DURBIN, P. A. 1981 Distorted turbulence in axisymmetric flow. *Q. J. Appl. Maths* **34**, 489–500.
- DURBIN, P. A. 1993 A Reynolds stress model for near-wall turbulence. *J. Fluid Mech.* **249**, 465–498.
- GIBSON, M. M. & LAUNDER, B. E. 1978 Ground effects on pressure fluctuations in the atmospheric boundary layer. *J. Fluid Mech.* **86**, 491–511.
- GOLDSTEIN, M. E. & DURBIN, P. A. 1980 The effect of finite turbulence spatial scale on the amplification of turbulence by a contracting stream. *J. Fluid Mech.* **98**, 473–508.
- GRADSHTEYN, I. S. & RYZHIK, I. M. 1980 *Table of Integrals, Series and Products*. Academic.
- HANJALIC, K. & LAUNDER, B. E. 1976 Contribution towards a Reynolds-stress closure for low-Reynolds-number turbulence. *J. Fluid Mech.* **74**, 93–610.
- HANNOUN, I. A., FERNANDO, H. J. S. & LIST, E. J. 1988 Turbulence structure near a sharp interface. *J. Fluid Mech.* **189**, 189–209.
- HUNT, J. C. R. 1973 A theory of turbulent flow round two-dimensional bluff bodies. *J. Fluid Mech.* **61**, 625–706.
- HUNT, J. C. R. 1984 Turbulence structure in thermal convection and shear-free boundary layers. *J. Fluid Mech.* **138**, 161–184.
- HUNT, J. C. R. & CARLOTTI, P. 2001 Statistical structure at the wall of the high Reynolds number turbulent boundary layer. *Flow, Turb. Combust* **66**, 453–475.
- HUNT, J. C. R. & CARRUTHERS, D. J. 1990 Rapid distortion theory and the 'problems' of turbulence. *J. Fluid Mech.* **212**, 497–532.
- HUNT, J. C. R. & GRAHAM, J. M. R. 1978 Free stream turbulence near plane boundaries. *J. Fluid Mech.* **84**, 209–235 (referred to herein as HG).
- KIT, E. L. G., STRANG, J. & FERNANDO, H. J. S. 1997 Measurement of turbulence near shear-free density interfaces. *J. Fluid Mech.* **334**, 293–314.
- KUMAR, S., GUPTA, R. & BANERJEE, S. 1998 An experimental investigation of the characteristics of free-surface turbulence in channel flow. *Phys. Fluids* **10**, 437–456.
- LAUNDER, B. E., REECE, G. J. & RODI, W. 1975 Progress in the development of a Reynolds-stress turbulence closure. *J. Fluid Mech.* **68**, 537–565.
- MCDUGALL, T. J. 1979 Measurements of turbulence in a zero-mean-shear mixed layer. *J. Fluid Mech.* **94**, 409–431.
- MONIN, A. S. & YAGLOM, A. M. 1975 *Statistical Fluid Mechanics*, Vol. 2. MIT Press.

- NAGANO, Y. & TAGAWA, M. 1988 Statistical characteristics of wall turbulence with a passive scalar. *J. Fluid Mech.* **196**, 157–185.
- NAGANO, Y. & TAGAWA, M. 1990 A structural turbulence model for triple products of velocity and scalar. *J. Fluid Mech.* **215**, 639–657.
- NAGAOSA, R. 1999 Direct numerical simulation of vortex structures and turbulent scalar transfer across a free surface in a fully developed turbulence. *Phys. Fluids* **11**, 1581–1595.
- NAKAGAWA, H. & NEZU, I. 1977 Predictions of the contributions to the Reynolds stress from the bursting events in open-channel flows. *J. Fluid Mech.* **80**, 99–128.
- PAN, Y. & BANERJEE, S. 1995 A numerical study of free surface turbulence in channel flow. *Phys. Fluids* **7**, 1649–1664.
- PEROT, B. & MOIN, P. 1995a Shear-free turbulent boundary layers. Part 1. Physical insights into near-wall turbulence. *J. Fluid Mech.* **295**, 199–227 (referred to herein as PM).
- PEROT, B. & MOIN, P. 1995b Shear-free turbulent boundary layers. Part 2. New concepts for Reynolds stress transport equation modelling of inhomogeneous flow. *J. Fluid Mech.* **295**, 229–245.
- RASHIDI, M. 1997 Burst-turbulence interactions in free surface turbulent flows. *Phys. Fluids* **9**, 3485–3501.
- RISSO, F. & FABRE, J. 1997 Diffusive turbulence in a confined jet experiment. *J. Fluid Mech.* **337**, 233–261.
- SHEN, L., ZHANG, X., YUE, D. K. P. & TRIANTAFYLLOU, G. S. 1999 The surface layer for free-surface turbulent flows. *J. Fluid Mech.* **386**, 167–212.
- SHIH, T. H. & LUMLEY, J. L. 1986 Second-order modelling of near-wall turbulence. *Phys. Fluids* **29**, 971–975.
- TENNEKES, N. H. & LUMLEY, J. L. 1972 *A First Course in Turbulence*. MIT Press.
- TEIXEIRA, M. A. C. & BELCHER, S. E. 2000 Dissipation of shear-free turbulence near boundaries. *J. Fluid Mech.* **422**, 167–191.
- THOMAS, N. H. & HANCOCK, P. E. 1977 Grid turbulence near a moving wall. *J. Fluid Mech.* **82**, 481–496.
- TOWNSEND, A. A. 1976 *The Structure of Turbulent Shear Flow*. Cambridge University Press.
- TURFUS, C. & HUNT, J. C. R. 1987 A stochastic analysis of the displacements of fluid elements in inhomogeneous turbulence using Kraichnan's method of random modes. In *Advances in Turbulence* (ed. Comte-Bellot & Mathieu), pp. 191–203. Springer.
- UZKAN, T. & REYNOLDS, W. C. 1967 A shear-free turbulent boundary layer. *J. Fluid Mech.* **28**, 803–821.
- VEERAVALLI, S. & WARHAFT, Z. 1989 The shearless turbulence mixing layer. *J. Fluid Mech.* **207**, 191–229.
- WALKER, D. T., LEIGHTON, R. I. & GARZA-RIOS, L. O. 1996 Shear-free turbulence near a flat free surface. *J. Fluid Mech.* **320**, 19–51 (referred to herein as WLGR).
- WONG, H. Y. W. 1985 Shear free turbulence and secondary flow near angled and curved surfaces. PhD Dissertation, Cambridge University.